QUARTERLY PROGRESS REPORT NO. 20

ON

CONTRACT NASr-7

For the Period

July 1, 1965 through September 30, 1965

Project

HYPERVELOCITY IMPACT OF MICROPARTICLES

F. C. Todd, Principal Investigator
Lin Wang, Graduate Research Assistant

Presented by

Research Foundation
Oklahoma State University
Stillwater, Oklahoma

Marvin T. Edmison, Ph.D. Director

ANALYTICAL CONSIDERATIONS ON THE PROPAGATION OF A SHOCK THROUGH FLUID, PLASTIC AND ELASTIC MEDIA

INTRODUCTION

The attached report is submitted as the twentieth Quarterly Progress Report on Project NASr-7. The title of the project is "Shock, Flow and Radiation from the Hypervelocity Impact of Microparticles". The analytical and experimental phases of this project are concerned with the phenomena that occur with the hypervelocity impact of microparticles on a massive target, which may be solid, or layered. The over-all objective is to obtain a sufficiently fundamental understanding of the physical mechanisms in the hypervelocity impact of a microparticle so that the momentum and energy transferred from the particle to the target may be ascertained, and possibly, the density of the incident microparticles may be estimated.

The attached report is a collection of references on the mechanisms by which the shock from a hypervelocity impact is propagated, almost radially, away from the zone of the impact. A report for an M.S. degree is a review of published information and a collection of references on the subject. It does not, necessarily, present new information. A report is considered to require less than one third of the time to prepare that would be required for a thesis and is usually, but not necessarily, used for terminal degrees.

With velocities that are high in the hypervelocity range for the impact of a microparticle, the pressure in the target and in the adjacent

missile material may reach the magnitude of a few to perhaps 50 megabars. In this pressure range, the materials are considered to flow as a non-viscous fluid. As the shock front propagates into the target and away from the impacting missile, the shock changes shape and the area of the shocked front increases so the intensity of the shock decreases. As a very rough approximation, the decrease is inversely proportional to the square of the distance from the initial zone of impact. As the peak pressure decreases, the shock interaction with the target no longer produces a fluid media, instead the media is only made plastic. With further decrease in amplitude of the shock front, the target material transmits the shock while remaining an elastic material. This report assembles the basic equations for the propagation of the shocks through these three media. It does not discuss the coupling of the shock from one media to another.

This report concludes with a short review of the Russian literature on the shock compression of porous media. There is still more recent American literature on the subject which substantiates most of the Russian conclusions, but which extends the explanation still further than is presented in this report. Work has been started to program the problem for the impact of a porous sphere onto a semi-infinite slab of aluminum. This computer program is to include the plastic and elastic material and is expected to be very, very long. This computation will include the effect of the change in media as the shock propagates away from the impact zone.

As a preliminary to this long, proposed investigation that is starting, the hypervelocity impact of thin plates of solid and of porous materials is being investigated. The major area of difficulty in this

particular phase is the reflection of the shock from the back faces of the impacting, thin plates. The treatment of shock reflection from the back face of the plate is difficult and is not entirely amendable to the mathematics of a continuum. The reflected shock ruptures the plate along irregular, non-plane interfaces of inherent weakness in the plate. The position of these interfaces is not predictable by a simple treatment of a continuum. The overall consequence of multiple rupture of the impacting plate is to convert a part of the initial kinetic energy of the plate into heat. An approximate method to allow for this conversion is being investigated.

ANALYTICAL CONSIDERATION ON THE PROPAGATION OF A SHOCK THROUGH FLUID, PLASTIC AND ELASTIC MEDIA

By

LIN WANG

Bachelor of Science

National Taiwan University

Taipa, Taiwan, China

1956

Submitted to the Faculty of the Graduate School of
the Oklahoma State University
in partial fulfillment of the requirements
for the degree of
MASTER OF SCIENCE
May, 1966

Name: Lin Wang Date of Degree: May 22, 1966

Institution: Oklahoma State University Location: Stillwater, Oklahoma

Title of Study: CONSIDERATIONS ON SHOCK PROPAGATION THROUGH FLUID, PLASTIC AND ELASTIC MEDIA

Pages in Study: 65 Candidate for Degree of Master of Science

Major Field: Physics

Scope and Method of Study: This report presents the basic considerations, boundary conditions and equations that are required to calculate the propagation of a radial shock away from the point of a hypervelocity impact. A hypervelocity impact is defined as the collision of two bodies that are approaching faster than the velocity of sound in either body. Examples of hypervelocity impacts are the incidence of micrometeroids on space vehicles. With very large velocities in the hypervelocity impact, the volume of affected material is initially very small and maximum pressure of 40 megabars are calculated. At these pressures, all materials are believed to behave as non-viscous fluids. As the almost radial shock propagates away from the impact zone, the shock pressure will decrease and the material will only be made plastic by the shock and, eventually, it remains elastic. This report presents the equations for the solution of shock propagation through fluid, plastic and elastic media.

Findings and Conclusions: Equations exist, have been published and are generally accepted for the calculation of the propagation of a shock through three types of media; fluid, plastic and elastic. The splitting of the single shock in the fluid region into two separate shocks that propagate at different velocities is discussed.

ADVISER'S APPROVAL _____

ACKNOWLEDGMENTS

This work was undertaken at the suggestion of Dr. F. C. Todd who acted as my adviser and project supervisor. The purpose of this study is to collect and present the basic concepts and equations for the propagation of a spherical shock in fluid, plastic and elastic media.

The assistance and guidance of Dr. Todd have been invaluable in the completion of this work.

The work was carried out under NASA Contract Number NASr-7, administered through the Research Foundation, Oklahoma State University.

TABLE OF CONTENTS

LIST OF TABLES

LIST OF FIGURES

LIST OF FIGURES (Continued)

CHAPTER I

INTRODUCTION

The objective of the following study is to collect and to present a summary of the published concepts and equations for the last phase in the solution of the problem of radial shock propagation from the hypervelocity impact of a sphere on a semi-infinite slab. An impact is defined as in the hypervelocity range when the incident body approaches the impact surface at a velocity that is in excess of the velocity of sound in the target material. Preceding theses on this project have considered the earlier phases of the impact. The present report will concentrate on the last phases of the impact in which spherical shock makes the transition from propagating through the self-produced fluid region, into the self-produced plastic region and, finally, into the elastic region. The last named region is the one in which the energy input into the material of the target from the passage of the shock is too small to convert the elastic properties of the target material into the plastic range.

In the collection of information for this report, the discussion includes several related subjects. In the following, the propagation of a shock through an inviscid fluid is considered in some detail. This is followed by a discussion of shock propagation through a plastic and through an elastic material. In considering these types of shock propagation, several subjects will be particularly emphasized. In the

discussion of shock propagation through the plastic media, the elastic-plastic model will be discussed since this explains the separation of the shock into a fluid shock and into an elastic precursor to the fluid shock. In the discussion of elastic shock waves, the static and dynamic elastic limits are differentiated and discussed. In addition, the contribution of the Bauschinger effect in increasing the dynamic-elastic limit is discussed. Equations of state are presented which are to be the preliminary basis for covering the elastic, plastic and fluid regions for iron and aluminum. Some proposed equations of state for special materials are mentioned.

CHAPTER II

DISCUSSION OF THE INVISCID, HYDRODYNAMIC MODEL FOR HYPERVELOCITY IMPACT

Bethe (1) has shown that the propagation of a shock front through any meterial may be calculated provided that the equation of state for the material is known over the pressure range under investigation. There are only three limitations on this statement, and these will be considered and amplified later in this report. For pressures in excess of a few megabars, it has been customary to obtain the solution by employing the hydrodynamic equations for non-viscous flow (2). The mathematical techniques are available to solve any problem of shock propagation through an inviscid medium provided five equations are known. As mentioned above, the equation of state must be known. The equations for inviscid, hydrodynamic flow consist of three equations which are for the conservation of mass, momentum and energy. The fifth and last requirement is that the entropy must increase across the shock front.

In the part of this report, the propagation of a shock is considered for a region which is considered to be a non-viscous fluid. This discussion is presented under three different headings. (a) There will be a detailed consideration of the shock front and the equations that relate the condition of the material on both sides of the shock front. (b) The equations of state will be considered for several materials, but there will be emphasis on the equation of state for

aluminum. It developes that the easiest way in which to include the condition that the entropy increases across the shock front is to formulate the equation of state in terms of the Hugoniot curve. This curve gives the final state of the material that has been compressed by a shock front. This is a direct and effective way to include the increase in entropy by the compressive shock. (c) For completeness of the treatment, the equations for hydrodynamic flow are listed. For calculations with a computer, J. von Neumann and R. D. Richtmyer (3) have shown that the solution without a discontinuity may be obtained by the introduction of a pseudo-viscosity term that has two effects. It damps out the computer induced oscillations in the solution, and it spreads the sudden pressure increase in the shock front over a fictitious width of two, to four of the mesh sizes that are used for the computer solution.

Rankine-Hugoniot Conditions

In the preceding introduction, it was indicated that five equations are sufficient to calculate the propagation of a shock wave. These equations are not sufficient, without other considerations, to define the conditions in the shock front. They are sufficient, however, to relate the conditions in the medium just before the shock wave reaches the medium to the conditions in the medium just after the shock front has passed. These equations may be derived from the flow equations, or they may be derived from basic considerations. They are so useful that they are designated the Rankine-Hugoniot relations. The thermodynamic significance of the equations is considered in order to show that the increase in entropy across the shock front can be shown on a

plot of the pressure vs the volume.

The shock wave concept is concisely illustrated by consideration of the following idealized situation. Suppose a uniform pressure, P_1, is suddenly applied to the entire surface of a thick slab of a compressible material, as shown in Figure 1. The signal that this pressure has been applied is transmitted to the interior of the slab by means of a stress wave. The material under shaded area is suddenly compressed to a pressure, P_1. If the compressibility of the material decreases with increasing pressure, that is to say if the material behaves normally in compression like most solid material, the wave front S will be essentially a discontinuity in stress, density, material velocity, and internal energy. The stress wave travels at supersonic velocity, with respect to the undisturbed material ahead of it. Only at the limit as P_1 approaches zero does its velocity become sonic. Except in the sonic limit, S is called a shock front.

If the pressure P_1 remains constant during the time of observation, the variables characterizing the shocked material including stress P_1, density ρ_1, internal energy E_1, and material velocity u_1, are constant between the boundary B and the shock front S. The relations between these variables and their values in the undisturbed material ahead of S can be described by the Rankine-Hugoniot jump conditions, or simply jump conditions, supplemented by an equation of state for the material. These jump conditions are the equations expressing the principles of the conservation of mass, of momentum and of energy across the shock front. They may be derived directly from the equations for hydrodynamic flow (4). The jump conditions may be shown to hold for any geometry, independent of the curvature of the shock front (5); hence a derivation

of the jump conditions directly from the conservation principles will be given for a plane front. It is also necessary to assume that thermodynamic equilibrium exists in both the compressed and the undisturbed material.

To derive the relation for the conservation of mass, consider a tube of material along the direction of flow and with unit cross-sectional area normal to the direction of wave propagation. The tube is shown by ABCD in Figure 2. It starts in the compressed material and ends in the uncompressed material. The principle of conservation of mass is expressed by observing that in a short period of time, dt, the shock front S travels a distance Udt, while the material which was initially at the plane, S, has traveled only a distance $u_1 dt$. During this flow, the material of mass $\rho_o U dt$, which is encompassed by the shock during the time interval, dt, has been compressed into a space $(U-u_1)dt$ at a density ρ_1. Since mass is conserved, the following relation must follow:

$$\rho_o U = \rho_1 (U-u_1) . \tag{1}$$

The equation expressing the principle of conservation of momentum across the shock front is obtained by reference to the same reactangle. The force acting on the material contained in the tube ABCD of unit cross-sectional area is, from the left across the plane AD in the shock state, P_1, and from the right P_o, which is the ambient pressure. The net force across the unit area is P_1-P_o to the right. In the time interval, dt, the mass of the material encompassed by the shock is $\rho_o U dt$, and this much mass is accelerated from rest to a velocity of u_1. The increase in momentum of the system is then $\rho_o U u_1 dt$, and the rate of

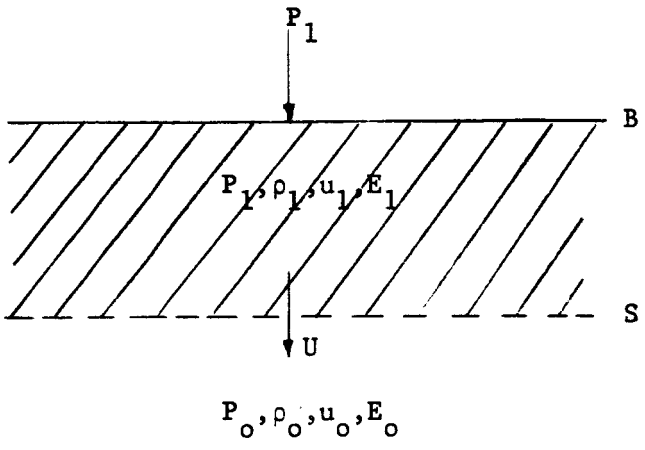

Fig. 1. Shock Wave in a Slab of a Compressible Material.

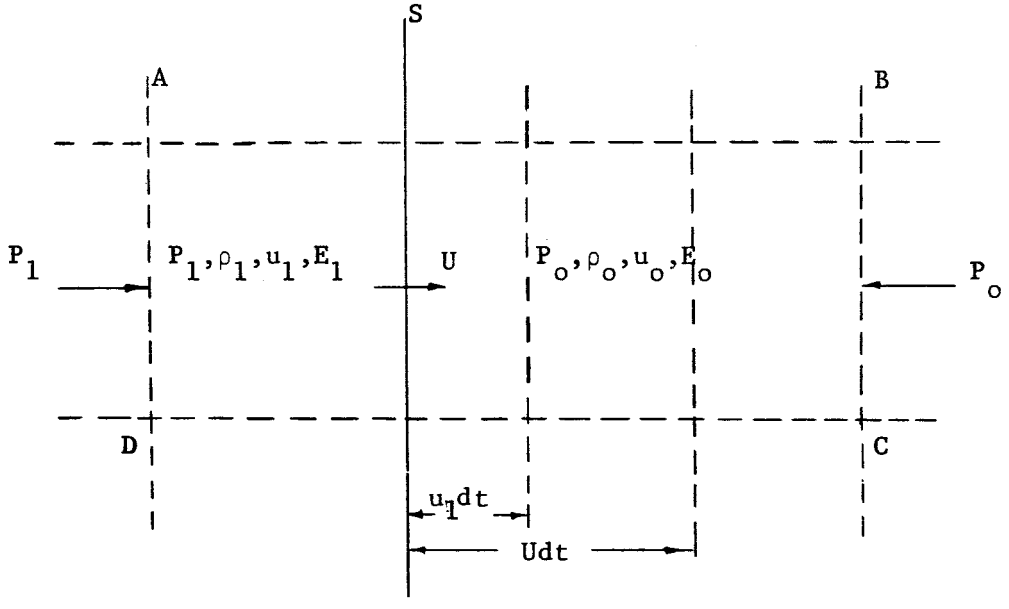

Fig. 2. Progress of a Plane Shock Wave.

change of momentum is given by dividing by the time interval, dt; thus the following equation follows:

$$P_1 - P_o = \rho_o U u_1 \tag{2}$$

The expression for the principle of conservation of energy across the shock front is obtained in a similar way. The plane AD advances a distance $u_1 dt$ during the time dt, so the work done on mass contained in the tube of unit cross-sectional area is $P_1 u_1 dt$. This amount of work must be equal to the sum of the increase of kinetic and internal energy of the system. The increase in kinetic energy is equal to $\frac{1}{2}(\rho_o U dt) u_1^2$ and the increas in internal energy is $(E_1 - E_o)\rho_o U dt$, where E_1 and E_o are specific internal energy of shocked and unshocked material, respectively. Equating the work done to the gain in energy of the system gives the energy equation across the shock front.

$$P_1 u_1 = \tfrac{1}{2}\rho_o U u_1^2 + \rho_o U(E_1 - E_o) \tag{3}$$

Combining Equations 1 to 3, to eliminate U and u_1, yields the Rankine-Hugoniot relation.

$$E_1 - E_o = \tfrac{1}{2}(V_o - V_1)(P_1 + P_o) \tag{4}$$

Where $V \equiv 1/\rho$ is the specific volume of the material. It is worthwhile to note that Equation 4 correlates only the thermodynamic variables of the material ahead of the shock front and behind the shock front. Equations 1, 2, and either 3 or 4 are the jump conditions which must be satisfied by material parameters on the two sides of the shock front. A rather detailed derivation for the above equations can be found in Courant and Freidrich's book (6).

When the shock transition, shock front, or simply shock, connects

a uniform, undisturbed state with a uniform shocked state, as in the case just described, it can be precisely defined. In co-ordinates fixed with respect to the shock front the transition zone is the region between two uniform, moving thermodynamic states of the medium. Material is flowing into the transition region at supersonic velocity and out at subsonic velocity.

While this definition is essential to understanding the basic physical nature of the shock transition, the conceptual realization of two uniform states, connected by a steady transition, is hard to achieve. For this reason, the meaning of the word "shock" is extended to include cases where stress and density change abruptly from one value to another, even though one or both of the connected states may be changing with time (7). These waves may be called "non-uniform" shock waves, and a typical profile is shown in Figure 3. In the illustration, region I is steady but region III is not. The boundary, A, between II and III is changing with time because region III consists of a relief or expansion wave which propagates at a higher speed than the shock in region II (8). The state at A differs, in general, from that which would obtain if III were a uniform state. It is customary to say that states A and I are connected by a shock transition although this is not precisely true. The accuracy of the approximation increases as the ratio of the magnitude of the pressure gradient in region II to that in region III increases, becoming exact when the transition is discontinuous.

Thermodynamic Considerations of the Shock Front

In the following paragraphs a brief discussion of the thermodynamics

of the shock transition will be given. The shock transition imparts both kinetic and internal energy to the material through which it propagates. Furthermore, irreversible work is done on the material as it passes through the shock front. This can be readily shown by using the Rankine-Hugoniot relation, Equation 4. Consider two shock waves propagating through two separate specimens of the same material. One shock has a pressure, P_1, and the other has a pressure, $P_1 + dP_1$. Each is supposed to be propagating into material in the same state, (P_o, V_o). Then the difference in specific internal energies behind the two shock fronts is found by differentiating Equation 4:

$$dE_1 = \tfrac{1}{2}(V_o - V_1)\,dP_1 - \tfrac{1}{2}(P_1 + P_o)\,dV_1 \qquad (5).$$

Since both states are assumed to be in thermodynamic equilibrium, the change of entropy may be calculated from the combined first and second laws of thermodynamics:

$$T_1 dS_1 = dE_1 + P_1 dV_1 \qquad (6).$$

Substitute dE_1 from Equation 5 into 6,

$$T_1 dS_1 = \tfrac{1}{2}(V_o - V_1)\,dP_1 + \tfrac{1}{2}(P_1 - P_o)\,dV_1 \qquad (7).$$

In order to convert Equation 7 into a more convenient from for discussion, the following two relations are introduced

$$C_1^2 = V_1^2 \frac{dP_1}{dV_1} \qquad (8).$$

and

$$(U - u_1)^2 = V_1^2 (P_1 - P_o)/(V_o - V_1) \qquad (9).$$

The latter relation may be obtained by combining Equations 1 and 2.

Equation 8 may be rewritten as

$$dV_1 = \frac{V_1^2}{C_1^2} dP_1 \qquad (10).$$

The following relation follows from Equation 9,

$$(P_1 - P_o) = \frac{1}{V_1^2} (U - u_1)^2 (V_o - V_1) \qquad (11).$$

Substitution of Equation 10 and 11 into Equation 7 yields

$$T_1 dS_1 = \tfrac{1}{2}(V_o - V_1)\left[1 - \left(\frac{U - u_1}{C_1}\right)^2\right] dP_1 \qquad (12).$$

The locus of all states (P_1,V_1) which can be obtained by a shock transition from an initial state (P_o,V_o) is called the Rankine-Hugoniot curve. Sometimes it is called R-H curve. Since this curve is concave upward, as shown in Fig. 4, it is clear from Equations 10, 11 and 12 that $dS_1>0$. The ratio $(U - u_1)^2/C_1^2$ is the absolute value for the slope of the Rayleigh line which is defined as the chord drawn between (P_o,V_o) and (P_1,V_1), divided by the tangent to the curve at (P_1,V_1). Since (P_1,V_1) is an arbitrary point on the R-H curve, the entropy, S, increases monotonically with pressure, P_1, and consequently, the R-H curve lies above the adiabat passing through the initial state, as shown in Fig. 4. The two curves have the same slope and curvature at the initial state A. It is also a straightforward, thermodynamic claculation to show that the entropy change is the third order in compression (9):

$$S_1 - S_o = \frac{1}{12T_o} \left(\frac{\partial^2 P}{\partial V^2}\right)_{S_o,V_o} (V_1 - V_o)^3 + \text{-----} \qquad (13).$$

Where S_o and T_o are the entropy and temperature of the initial state, An expression, in closed form, for Equation 13 may be obtained if an

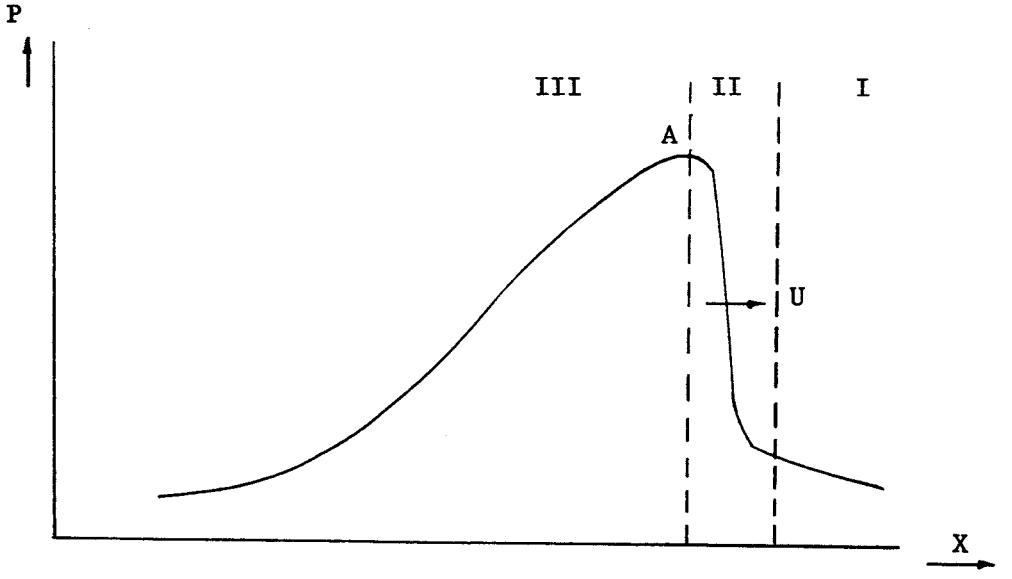

Fig. 3. Profile of a Nonuniform Shock.

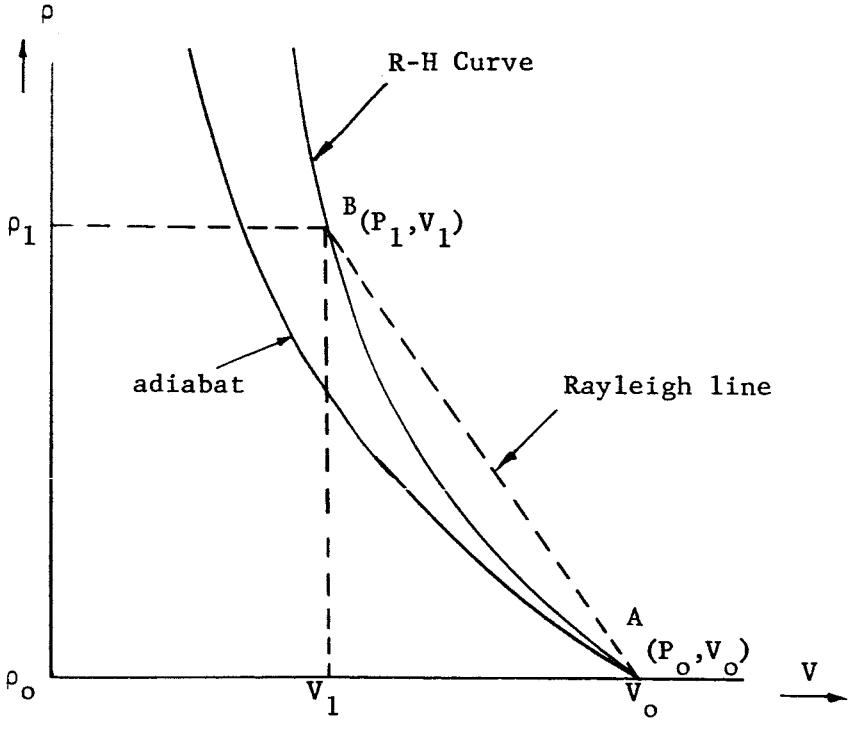

Fig. 4. Comparison of Hugoniot Curve and Adiabat.

equation of state is given (10).

Equations of State

Bethe has shown that the equations for the propagation of shock may be solved provided an equation of state is known for the pressure range and provided the following three conditions are satisfied.

1. $\left(\frac{\partial^2 P}{\partial V^2}\right)_S > 0,$

2. $V\left(\frac{\partial P}{\partial E}\right)_V > -2,$

3. $\left(\frac{\partial P}{\partial V}\right)_E < 0.$

In these expressions P is the pressure, V the specific volume, E the specific internal energy, and S is the entropy. It was observed that these three conditions are satisfied for all known materials which do not undergo a change of phase over the pressure range associated with the shock wave under investigation.

The Equation of State for Aluminum

The equation of state for aluminum was a composite from various published data that was prepared by Mr. B. A. Sodek. It was found to give satisfactory results for calculation on the propagation of a shock through a fluid when the hydrodynamic flow equations were used. Since the solution of the hydrodynamic flow equations are found with a digital computer, it is possible to express the equation of state for the whole range of pressures associated with the shock wave. Several different equations, each of which is good for a certain range, are combined to

cover the whole pressure range of the shock.

The equation of state for aluminum, in the Mie-Gruneisen form, is

$$P - P_h = \rho\gamma(\epsilon - \epsilon_h) \tag{14}$$

where P is the pressure, ρ is the density, and ϵ is the specific internal energy. The pressure, P_h, and the specific internal energy, ϵ_h, are known functions of the specific volumes over the pressure range, for which the Hugoniot curve for the material is known. The symbol γ is called the Gruneisen ratio. It is a function only of the specific volume; thus, the Mie-Gruneisen equation is a complete thermodynamic description of a P, V, ϵ equation of state for the material.

For computations on a computer, the Hugoniot curve in this report was divided into three pressure ranges. It was constructed by using the published experimental data of Walsh, et. al., (11,12) in the pressure range up to 1 Megabar, the published data of the Thomas-Fermi statistical model for pressure range above 20 Megabars, and an interpolation for the range between 1 Megabar and 20 Megabars. An effort was made to fit the pressure data for the Hugoniot curve to three analytical equations of the form, $P_h = A\mu + B\mu^2 + C\mu^3$. In the cubic polynomial A, B, and C are constants which are determined by the shape of the Hugoniot curve. The variable, $\mu = (\frac{V_o}{V} - 1) = (\frac{\rho}{\rho_o} - 1)$, is defined with V_o and ρ_o as the specific volume and the density of aluminum in its unstrained state. In order to be able to use the same analytical form for the complete pressure range, three different sets of constants, A, B. and C are needed in the three separate ranges. The values for the constants A, B, and C and the specific volume ranges in which they are valid are listed in Table I. The Gruneisen ratio, γ in Equation 14,

TABLE I

CONSTANTS FOR THE HUGONIOT OF ALUMINUM

V/V_o	A	B	C	Pressure (in megabars)
1.0 to .650	765.0	1659.0	428.0	0 to 1.000
.650 to .518	1150.1	-851.9	3398.0	1.000 to 3.570
.518 to .300	-2194.2	4034.7	2604.3	3.570 to 52.000

TABLE II

CONSTANTS FOR GRUNEISE'S RATIO

V/V_o	γ_o	a	b	c	Pressure (in megabars)
1.0 to .650	2.130	-5.193	12.098	12.550	0 to 1.000
.650 to .518	2.000	-4.513	6.800	-3.780	1.000 to 3.570
.518 to .300	1.590	-1.355	.439	.0404	3.570 to 52.000

is regarded as a function of the specific volume. It was also approximated by a cubic polynomial of the form, $\gamma = \gamma_o + a\mu + b\mu^2 + c\mu^3$. The coefficients γ_o, a, b and c are evaluated in the three pressure ranges correspond to those ranges, in which A, B, and C are valid. The values are listed in Table II.

The Equation of State for Iron

The equation of state for iron was taken from the published data of R. L. Bjork (13). The equation has the following form:

$$P = [a_1\mu + a_2\mu|\mu| + e(b_o + b_1\mu + b_2\mu^2) + e^2(c_o + c_1\mu)]/(e + e_o)$$

The symbols in the above equation are listed below.

P = pressure

ρ = density

ρ_o = normal density of iron = 7.86 gm/cm^3 = 7.86 $megagram/m^3$

E = specific internal energy

$e = E\rho_o$

$\mu = \rho/\rho_o - 1.$

The values for the constants in the above equation are listed below:

$a_1 = 7.780 \times 10^4$

$a_2 = 31.18 \times 10^4$

$b_o = 959.1$

$b_1 = 1568$

$b_2 = 463.4$

$c_o = 0.3984$

$c_1 = 0.5306$

$e_o = 900$

The units used in the above equation are of meter, megagram and second.

Fundamental Equations of Hydrodynamic Flow

The pressures resulting from hypervelocity impact are of such a tremendously large value that the yield strength of the material is neglibibly small compared to the stresses in the material. Since the rigidity of the material involved is of little significance, the motion of the material can be adequately described by the partial differential equations governing the hydrodynamic flow of a compressible fluid.

As stated by Courant anf Friedrichs (14), the following system of partial differential equations and conditions are needed to give a complete description of the motion of the fluid except where a shock front exists.

1. The differential equation expressing the principle of conservation of mass, which is often called the continuity equation.

2. The differential equation expressing the principle of conservation of momentum, which is the equation of motion.

3. The differential equation expressing the principle of conservation of energy.

4. The condition that an equation of state of the fluid medium in the pressure range under study is available.

5. The condition that the change of state of the fluid medium is adiabatic except at the shock front.

The differential equations and conditions listed above, together with the initial and boundary conditions determine the solution to the

problem under consideration.

The differential equations which describe the fluid motion are usually written in either Eulerian, or Lagrangean form. In the Eulerian form, the independent space variables refer to the coordinates system that is fixed in space and through which the fluid moves. The physical quantities of interest, such as density, flow velocity, spacific energy, and pressure, are functions of a space variable and the time t. In the Lagragean form, the independent space variable refers to a coordinates system that is fixed in the moving fluid and that is undergoing the motion of the fluid. With this coordinate system, each selected small volume of the fluid is permanently identified by its Lagrangean variables, while the actual position in space is a dependent variable which is found from the solution. It is possible to obtain the differential equations for hydrodynamic flow in either the Eulerian, or the Lagragean form. In this report the Eulerian form is discussed. In the following paragraphs, the fundamental, Eulerian equations of hydrodynamic flow are listed.

Let $\vec{X}(x,y,z)$ denote the position vector in a Cartesian coordinate system. The properties of the fluid medium are characterized by the density, $\rho = \rho(\vec{X},t)$; the flow velocity, $u = u(\vec{X},t)$; the specific internal energy $\epsilon = \epsilon(\vec{X},t)$; and the pressure $p = p(\vec{X},t)$. The assumption is made that all body forces are negligible. These forces include gravity, heat conduction, viscosity and energy sources. With these definitions and restrictions, the principle of the conservation of mass is expressed by the following equation, which is also called the continuity equation:

$$\frac{\partial \rho}{\partial t} + \vec{u} \cdot \nabla \rho = -\rho \nabla \cdot \vec{u} \tag{15}$$

The principle of conservation of momentum is expressed by

$$\rho \frac{\partial \vec{u}}{\partial t} + \rho \vec{u} \cdot \nabla u = - \nabla p \tag{16}$$

The principle of conservation of energy is expressed by

$$\rho \frac{\partial \epsilon}{\partial t} + \rho \vec{u} \cdot \nabla \epsilon = - p \nabla \cdot u \tag{17}$$

In a problem of spherical symmetry, the dependent variables $\rho(\vec{X},t)$, $u(\vec{X},t)$, $p(\vec{X},t)$ and $(\vec{X},t)$ are functions of the radial distance, r, and the time, t. They can be represented respectively by $\rho(r,t)$, $u(r,t)$, $p(r,t)$ and $\epsilon(r,t)$. The Equations 15, 16, and 17 then take respectively the following forms:

$$\frac{\partial \rho}{\partial t} + u \frac{\partial \rho}{\partial r} = - \frac{\rho}{r^2} \frac{\partial}{\partial r} (r^2 u), \tag{18}$$

$$\rho \frac{\partial u}{\partial t} + \rho u \frac{\partial u}{\partial r} = - \frac{\partial p}{\partial r}, \tag{19}$$

and

$$\rho \frac{\partial \epsilon}{\partial t} + \rho u \frac{\partial \epsilon}{\partial r} = - \frac{p}{r} \frac{\partial}{\partial r} (ru) \tag{20}$$

To obtain mumerical solutions with the large computers, it is desirable to convert Equations 18, 19 and 20 into dimensionless equations.

Equation 18 may be rewritten as

$$\frac{\partial \rho}{\partial t} = - u \frac{\partial \rho}{\partial r} - \rho \frac{\partial u}{\partial r} - \frac{2\rho u}{r}$$

which is equivalent to

$$\frac{\partial \rho}{\partial t} = - \frac{1}{r^2} \frac{\partial}{2r} (r^2 \rho u). \tag{21}$$

Equation 19 may be rewritten as

$$\rho \frac{\partial u}{\partial t} = - \frac{\partial p}{\partial r} - \rho u \frac{\partial u}{\partial r}$$

By adding $u\frac{\partial \rho}{\partial t}$ to both sides of this equation, the following equation follows:

$$\rho \frac{\partial u}{\partial t} + u \frac{\partial \rho}{\partial t} = - \frac{\partial p}{\partial r} - \rho u \frac{\partial u}{\partial r} + u \frac{\partial \rho}{\partial t} .$$

By substitution of Equation 21 into this equation, the following equation is found.

$$\frac{\partial}{\partial t} (\rho u) = - \frac{\partial p}{\partial r} - \rho u \frac{\partial u}{\partial r} + u[- \frac{1}{r^2} \frac{\partial}{\partial r} (r^2 \rho u)].$$

This equation may be rewritten as

$$\frac{\partial}{\partial t} (\rho u) = - \frac{\partial p}{\partial r} - \frac{1}{r^2} \frac{\partial}{\partial r} (r^2 \rho u^2). \qquad (22)$$

Finally, Equation 20 can be rewritten as

$$\rho \frac{\partial \epsilon}{\partial t} = - \frac{p}{r^2} \frac{\partial}{\partial r} (r^2 u) - \rho u \frac{\partial \epsilon}{\partial r} .$$

Adding $\epsilon\frac{\partial \rho}{\partial t}$ to both sides of the above equation gives the following equation:

$$\rho \frac{\partial \epsilon}{\partial t} + \epsilon \frac{\partial \rho}{\partial t} = - \frac{p}{r^2} \frac{\partial}{\partial r} (r^2 u) - \rho u \frac{\partial \epsilon}{\partial r} + \epsilon \frac{\partial \rho}{\partial t}$$

Substitution of $\frac{\partial \rho}{\partial t}$ from Equation 21 into the above equation leads to the equation below,

$$\frac{\partial}{\partial t} (\rho \epsilon) = - \frac{p}{r^2} \frac{\partial}{\partial r} (r^2 u) - \rho u \frac{\partial \epsilon}{\partial r} + \epsilon[- \frac{1}{r^2} \frac{\partial}{\partial r} (r^2 \rho u)]$$

$$= - \frac{p}{r^2} \frac{\partial}{\partial r} (r^2 u) - \frac{1}{r^2} \frac{\partial}{\partial r} (r^2 \rho u \epsilon),$$

which may be rewritten as,

$$\frac{\partial}{\partial t}(\rho\epsilon) = -\frac{1}{r^2}\left[p\frac{\partial}{\partial r}(r^2u) + \frac{\partial}{\partial r}(r^2\rho u\epsilon)\right] \qquad (23)$$

Equations 21, 22 and 23 are in convenient forms to change into dimensionless equations.

The Artificial Dissipative Mechanism

At the shock front, the density, flow velocity, specific energy, and the pressure are all discontinuous. At the shock front, the differential equations must be replaced by the Rankine-Hugoniot jump conditions, which serve as internal boundary conditions in such a way that the conditions of the fluid on the two sides, behind and in front, of the shock front are related. These relations provide sufficient conditions to relate the differential equations on both sides of the shock front (15). The application of the jump conditions, as internal boundary conditions in solving the problem of shock propagation, is known as shock fitting. The process is really a complicated, iterative, trial-and-error method. A rather detailed discussion for feasible examples to use the shock fitting method was given by Richtmyer (16). In order to avoid using the shock fitting method, von Neumann and Richtmyer (3) devised an approximate method which is primarily for computer calculations. This method automatically calculates across the shock front for hydrodynamic flow problems, wherever they occur. The essence of the method is to replace the Hugoniot jump conditions in the calculations, with an artificial dissipative mechanism. Typical, naturally-occurring dissipative mechanisms are viscosity and heat conduction, which characterize a real fluid. The effects of the artificial dissipative mechanism are to tend to smooth the shocks, so that

the surface of discontinuity, across which the physical quantities of interest are discontinuous, is replaced by a thin transition layer in which the physical quantities of interest change abruptly, but continuously. With the incorporation of the artificial dissipative mechanism, or pseudo-viscosity, the differential equations describe the motion of the hydrodynamic flow in the transition layer as well as elsewhere in the flow. By introducing the artificial dissipative mechanism, the need to apply internal boundary conditions is avoided. The Rankine-Hugoniot conditions still remain true across the transition layer, which really is a widened shock front. The conditions required to select a suitable artificial dissipative term are listed below:

1. The introduction of the artificial pseudo-viscous term in the momentum and energy equations must have a negligible effect on the solutions of the hydrodynamic flow problem everywhere except across the transition layer.

2. The Rankine-Hugoniot jump conditions must remain true across the transition layer, so the hydrodynamic flow equations have solutions without any discontinuities.

3. The thickness of the transition layer must be independent of the shock strength and of the state of the material into which the shock is moving.

Various forms may and have been employed for the artificial pseudo-viscosity term, which is designated by Q. The specific form of the damping term is not important since it introduces a pseudo-damping effect to control the computer introduced oscillations. After trials by many investigators, one of the most useful forms is

$$Q = C\rho\left|\frac{\partial u}{\partial r}\right|\frac{\partial u}{\partial r}$$

This form for the Q-term was suggested by Richtmyer (17). This form produces damping that is proportional to the square of the velocity gradient. This is desirable for it quickly damps the computer generated osciallations. The use of the absolute value on one gradient is necessary to damp out both increasing and decreasing velocity gradients.

Dimensionless Differential Equations

In order that the numerical values of the variables will be within the numerical range of the digital computer, all of the variables are scaled. A dimensionless form of the hydrodynamic flow equations would also be highly desirable to permit easy scaling of problems for different initial values.

Let D, U, E, P, T, and R denote the density, flow velocity, specific internal energy, pressure, time, and radial distance, respectively, in the dimensionless hydrodynamic flow equations. The Equations 21, 22 and 23 are made dimensionless as shown in the following table.

$$\rho = \rho_o D. \tag{24}$$

$$u = C_o U. \tag{25}$$

$$\epsilon = e_o E. \tag{26}$$

$$p = p_o P. \tag{27}$$

$$t = t_o T. \tag{28}$$

$$r = r_o R. \tag{29}$$

In these relations, ρ_o, C_o, e_o, p_o, t_o and r_o are the scaling factors for each variable, as indicated. The substitution of the relations in 24, 25, 28 and 29 into Equation 21 yields the following equations:

$$\frac{\partial(\rho_o D)}{\partial(t_o T)} = - \frac{1}{(r_o R)^2} \frac{\partial}{\partial(r_o R)} (r_o^2 R^2 \rho_o D C_o U),$$

which may be rewritten as

$$\frac{\partial D}{\partial T} = - \frac{C_o t_o}{r_o} \frac{1}{R^2} \frac{\partial}{\partial R} (R^2 D U). \tag{30}$$

By substituting the relations in 24, 25, 27, 28 and 29 into Equation 22, the following equation is obtained.

$$\frac{\partial(\rho_o D C_o U)}{\partial(t_o T)} = - \frac{\partial(p_o P)}{\partial(r_o R)} - \frac{1}{r_o^2 R^2} \frac{\partial(r_o^2 R^2 \rho_o D C_o^2 U^2)}{\partial(r_o R)}$$

This may be rewritten as

$$\frac{\partial(DU)}{\partial T} = - \frac{p_o}{\rho_o} \frac{1}{C_o} \frac{t_o}{r_o} \frac{\partial P}{\partial R} - \frac{C_o t_o}{r_o} \frac{\partial(R^2 D U^2)}{\partial R} \tag{31}$$

For the energy equation, Equation 23, the substitution of the relations in 24, to 29 gives the following:

$$\frac{\partial(\rho_o D e_o E)}{\rho(t_o T)} = - \frac{1}{r_o^2 R^2} \left[p_o P \frac{\partial(r_o^2 R^2 C_o U)}{\partial(r_o R)} + \frac{\partial(r_o^2 R^2 \rho_o D C_o U e_o E)}{\partial(r_o R)} \right]$$

Simplification of the above equation gives

$$\frac{\partial(DE)}{\partial T} = - \frac{C_o t_o}{r_o} \frac{p_o}{\rho_o e_o} \frac{P}{R^2} \frac{\partial(R^2 U)}{\partial R} - \frac{C_o t_o}{r_o} \frac{1}{R^2} \frac{\partial(R^2 D U E)}{\partial R} \tag{32}$$

In order to make Equations 30, 31 and 32 dimensionless it is necessary to employ the following relations between the scaling factors, ρ_o, C_o, e_o, p_o, t_o and r_o. These are:

$$\frac{C_o t_o}{r_o} = 1, \tag{33}$$

$$\frac{p_o}{\rho_o} = C_o^2, \tag{34}$$

and

$$\frac{P_o}{\rho_o e_o} = 1. \tag{35}$$

The values for the variables in the flow equations may be confined to almost any desired range by the selection of scaling factors that satisfy Equations 33, 34 and 35. For illustration, a set of scaling factors that have been found to be satisfactory are selected in the following manner. The selected values are certainly not unique. Choose the density, ρ_o, to be the value for aluminum under standard conditions; i.e., $\rho_o = 2.785$ grams per cm^3. Choose the reference pressure to be $p_o = 1$ kilobar. Then c_o and e_o are determined by Equations 34 and 35. Choose some arbitrary distance, r_o, for the part of the problem that is of interest, then Equation 19 and the already determined value for c_o will fix t_o. With the scaling factors selected, Equations 33, 34 and 35 may be used to convert Equations 30, 31 and 32 into the following dimensionless equations.

$$\frac{\partial D}{\partial T} = - \frac{1}{R^2} \frac{\partial}{\partial R} (R^2 DU), \tag{36}$$

$$\frac{\partial}{\partial T} (DU) = - \frac{\partial P}{\partial R} - \frac{\partial}{\partial R} (R^2 DU^2), \tag{37}$$

and

$$\frac{\partial}{\partial T} (DE) = - \frac{P}{R^2} \frac{\partial}{\partial R} (R^2 U) - \frac{1}{R^2} \frac{\partial}{\partial R} (R^2 DUE). \tag{38}$$

When the pseudo-viscous term, designated by Q, is inserted into Equations 37 and 38, the following two equations are obtained:

$$\frac{\partial}{\partial T} (DU) = - \frac{\partial}{\partial R} (P + Q) - \frac{\partial}{\partial R} (R^2 DU^2) \tag{39}$$

and

$$\frac{\partial}{\partial T}(DE) = -\frac{1}{R^2}(P + Q)\frac{\partial}{\partial R}(R^2U) - \frac{1}{R^2}\frac{\partial}{\partial R}(R^2DUE) \quad (40)$$

Equations 36, 37 and 38 are in the final forms. They may be readily differenced and employed in a computer program.

CHAPTER III

CONSIDERATIONS ON THE PROPAGATION OF SHOCKS THROUGH AN ELASTIC MEDIUM

In the preceding section, the propagation of shocks at extremely high pressures was considered. The pressures were so great that the mechanical properties of the solid state could be neglected. This is equivalent to the statement that a negligible error results by omission from consideration of the yield strength and the shear strength of the target in its original state. For pressures below the dynamic yield strength, the material is elastic. Shocks of small amplitude are transmitted through an elastic medium at constant velocity and with no permanent change in the physical structure of the medium.

The basic equations for the elastic propagation of small shocks is to be considered in this section. Small shocks are equivalent to sound waves. Since there is an exceedingly large backlog of information on the acoustic properties of solids, all necessary background information is available. The reason for the intense interest in this subject may not be immediately apparent when the basic problem is known to be hypervelocity impact. The reason for the interest becomes obvious, however, when it is recalled that the only possible mechanical measurements on the effect of a hypervelocity impact must be observations on the elastic motion of the metal that surrounds the point of a hypervelocity impact.

For a definitive discussion of the states of matter that occur during a hypervelocity impact, a simple experiment is selected to serve as an illustrative example. Consider the hypervelocity impact of a small particle, such as a sphere, on a target which has the shape of a hemisphere. The point of impact of the sphere is to be at the center of the hemisphere. An impact is defined as hypervelocity when the impacting body, or missile, approaches the target at a velocity which is greater than the velocity of sound in the elastic material of the target. Immediately after the start of the impact, the pressure is very high around the entering missile. As a consequence of the high pressure, the missile and the material of the target, that is within the shock front, may be considered to be a non-viscous fluid that was produced by the impact. The flow of this missile-produced, that the shock produced, fluid may be calculated with the equations of hydrodynamic flow that were considered in the first section of this report. As the roughly hemispherical shock continues to propagate away from the initial point of contact, the pressure in the shock front must decrease for the area of the shock front increases as the square of the distance from the point of impact. Eventually, the shock pressure will fall so low that it will no longer produce a fluid; instead the medium will become a shock-produced plastic. The propagation of the shock in this plastic region will be considered in the last section. As the hemispherical shock continues to propagate, the shock pressure will become so small that the pressure does not permanently change the initial, elastic characteristics of the medium. This elastic state of the target material is the one that is now to be discussed.

In the elastic state, the shock front is not distinguishable from

the propagation of a sound wave. As a consequence, the propagation of the shock follows the laws for the propagation of acoustic waves through the medium. This means that there is a longitudinal, or dilational wave like those in the fluid region. In the elastic region, however, the dilational wave propagate at an almost constant velocity, which is practically independent of their amplitude. Actually, the velocity must increase slightly with an increase in pressure. This is required for a stable shock wave by one of Bethe's three conditions and accurate measurements have shown it to be true. Since the shock wave front is not a true hemispherical wave, it will produce some shear; particularly near to the surface, where there will be transverse, or shear waves. These waves are called Rayleigh waves. The Rayleigh waves propagate slower than the dilational waves; that is, at approximately 2/3 of the velocity of the dilational waves. They also decrease in amplitude exponentially with the depth.

Bethe's proof that the shock propagation may be calculated from an equation of state for the material is valid, as indicated above. In the fluid range, the equation of state must be of the most general form with three variables; such as the pressure, the density and the internal energy. For low pressures, where the elastic and, to a limited extent, the plastic waves exist, the increase in entropy across the shock front is small enough to be neglected. As a consequence, the velocity of propagation may be calculated with considerable accuracy from a relation between the pressure and the density. With this assumption, the differential equation becomes linear and many solutions have been found with this basic assumption. In the following discussion, the manner of calculating the speed of propagation of the dilational and

the Rayleigh waves is shown.

Comments on Elastic Shock Waves and Their Stability

In contrast to fluids, solids resist shear so that the thermodynamic description of a solid, which involve many components of stress and strain, is much more complicated than that of a fluid. If attention is confined to plane longitudinal waves, which are moving normal to the faces of a slab, no shearing forces arise. In this example, there is an analogy between elastic solids and fluids. Solids are capable of elastic deformations under certain conditions, and of plastic changes in shape under others. The properties of materials which characterize them as elastic, or plastic, can be expressed mathematically by the relation that exists between the stress σ, and the strain ϵ:

$$\sigma = \sigma(\epsilon)$$

The above relation depends only on the nature of the material under consideration. A material is called elastic when the stress depends linearly on the strain. Most material are elastic when the strain does not exceed a certain limit, which is called the critical strain. A material is called plastic when the stress is nonlinear function of the strain and this only occurs when the strain is greater than the critical strain.

For most solids, the compressibility decreases as pressure increases in adiabatic compression, so that the adiabat for hydrostatic compression in the P-V diagram is concave upward; i.e., $(\partial^2 p/\partial V^2)_S > 0$. This is exactly Bethe's condition for which compressive shocks are stable (1). The decrease in compressibility for solids with increasing pressure was shown by Bridgman (18). When dilational waves of large amplitude are

propagated through solids, shock waves result. The elastic waves of dilation are propagated through a solid with the velocity $[(\lambda + 2\mu)/\rho]^{\frac{1}{2}}$; or, when expressed in terms of the bulk modulus K, the velocity is $[(K + 4\mu/3)/\rho]^{\frac{1}{2}}$. It follows from the general theory (19), that this is also the velocity at wnich a purely dilational spherical wave will propagate in a solid for which Lame's constants are λ, μ, and the bulk modulus is K. As a result of the decrease in compressibility with increasing pressure, Bethe's condition for the formation of a stable shock wave is fulfilled. In other words, tne increase in the bulk modulus, K, with an increase in pressure dominates the expression for tne velocity, $[(K + 4/3\ \mu)/\rho]^{\frac{1}{2}}$; and results in an increase in the velocity of the elastic wave with pressure. This is the intrinsic requirement of Bethe's condition.

Propagation of a Spherical Elastic Shock

The case is discussed of a spherical elastic disturbance which propagates in a solid with tne Lame's elastic constants and λ, μ and with a bulk modulus, K. The coordinate system together with the related stress and strain components are shown in Figure 5. All physical quantities of interest are functions of the coordinates, r and t, as in the fluid region. Let σ_r, σ_t, ϵ_r and ϵ_t be radial and tangential components of stress and strain, respectively. Let u be the particle displacement. The strains are defined by

$$\epsilon_r = \frac{\partial u}{\partial r} , \tag{1}$$

$$\epsilon_t = \frac{u}{r} . \tag{2}$$

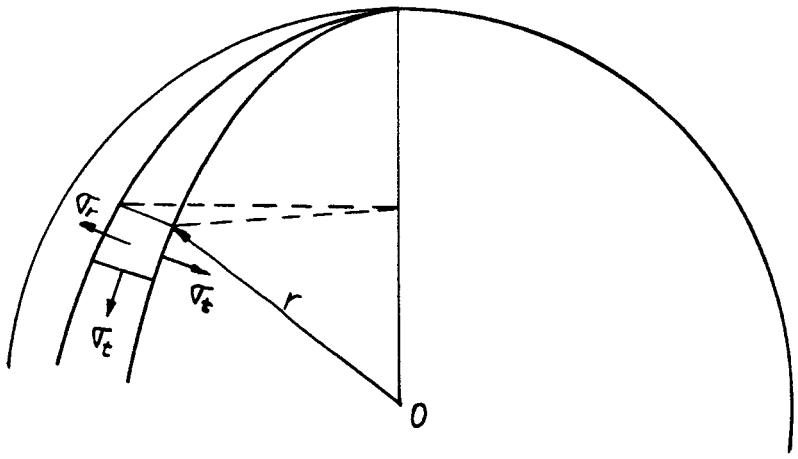

Fig. 5. Co-ordinate System and Stress Components.

The stresses and strains in elastic region are related by Hooke's law:

$$E \frac{\partial u}{\partial r} = \sigma_r - 2v\sigma_t, \tag{3}$$

$$E \frac{u}{r} = (1 - V)\, \sigma_t - V\sigma_r \tag{4}$$

From Equations 3 and 4, σ_r and σ_t are expressed by

$$\sigma_r = \frac{E}{(1 + \nu)(1 - 2\nu)} \left[(1-\nu) \frac{\partial u}{\partial r} + 2\nu \frac{u}{r}\right], \tag{5}$$

$$\sigma_t = \frac{E}{(1 + \nu)(1 - 2\nu)} \left[\frac{u}{r} + \nu \frac{\partial u}{\partial r}\right] \tag{6}$$

The equation of motion is

$$\frac{\partial \sigma_r}{\partial r} + \frac{2}{r} (\sigma_r - \sigma_t) = \rho \frac{\partial^2 u}{\partial t^2} \tag{7}$$

The elimination of the stresses among Equations 5, 6 and 7 results in an equation for u, as below:

$$\frac{\partial^2 u}{\partial r^2} + \frac{2}{r} \frac{\partial u}{\partial r} - \frac{2u}{r^2} = \frac{1}{C_e^2} \frac{\partial^2 u}{\partial t^2} \tag{8}$$

where C_e is given by

$$C_e^2 = \frac{(1 - \nu)E}{(1 + \nu)(1 - 2\nu)\rho} = \frac{\lambda + 2\mu}{\rho} = (K + 4/3\ G)/\rho. \tag{9}$$

In this expression, λ and μ are Lame's constants, K is the bulk modulus, $G(= \mu)$ is the shear modulus and ρ is the density. It is to be noted that the wave velocity depends upon tne shear modulus as well as on the bulk modulus. The physical reason for this is that the elements are subjected to a combination of tension and shear.

In dealing with shock waves in an elastic, or plastic material, as in the fluid region, certain internal boundary conditions must be

considered (20). At the shock front, the Rankine-Hugoniot conditions must be satisfied and, at the boundary between an elastic and a plastic region, the stresses and mass velocity must be continuous. After the particle displacement, u, is found as a function of r and t, the radial strain and stress may be found from Equations 1 and 5, respectively; the shear strain and stress may be found from Equations 2 and 6, respectively.

Rayleigh Waves

Only two types of elastic waves, dilational waves and shear waves, can be propagated in an unbounded isotropic solid. When there is a boundary surface, elastic surface wave may also occur. These surface waves, which are similar to gravitational surface waves in liquids, were first investigated by Lord Rayleigh; hence, they are called Rayleigh waves. It was found that their amplitude decreases rapidly with depth, and that their velocity of propagation is less than that of body waves.

Consider a sinusoidal surface, or Rayleigh, wave of frequency, f, velocity c, and wavelength Λ which is propagating along the surface in the x-direction. Take the direction toward the interior of the solid to be z-direction. The amplitudes of the stress components are designated σ_{xx} and σ_{zz}. It is desired to calculate the decrease in amplitude, u, in the x-direction and the decrease in amplitude, W, with deptn in the z-direction. For steel with a Poisson's ratio of 0.29, the calculated amplitude (21) are plotted in Figure 6. The curves are given in nondimensional forms, the peak value of displacements $\bar{u}$ and $\bar{w}$ being plotted as the ratios $\bar{u}/\omega_o$ and $\bar{w}/\omega_o$, where ω_o is the amplitude of the vibration in the z-direction at the surface. The peak values $\bar{\sigma}_{xx}$, $\bar{\sigma}_{yy}$

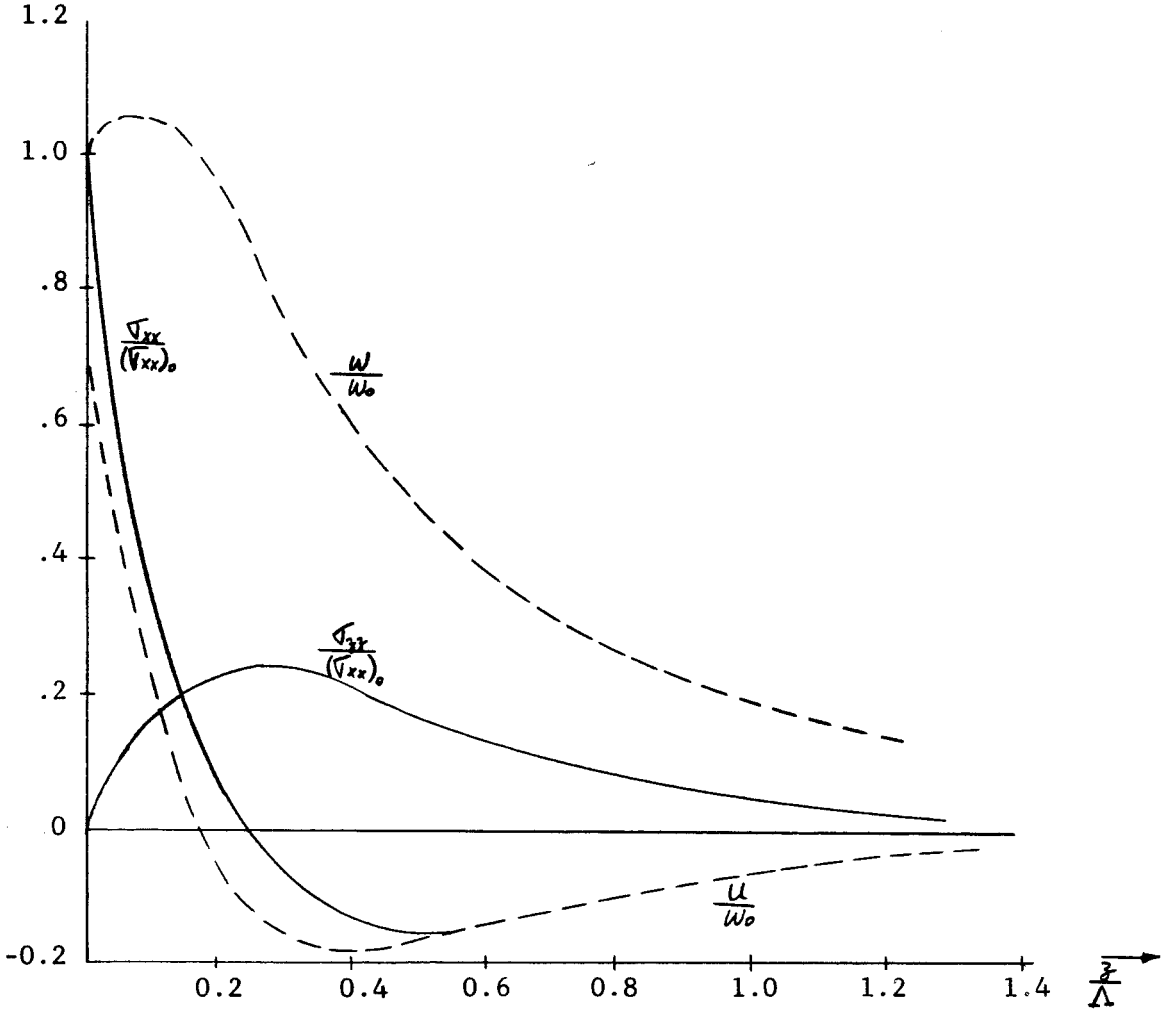

Fig. 6. Amplitudes of the Stresses and Displacement Associated with Rayleigh Surface Waves in Steel. V = 0.29.

of the stresses are plotted as the ratios $\sigma_{xx}/(\bar{\sigma}_{xx})_o$ and $\sigma_{zz}/(\bar{\sigma}_{xx})_o$, where $(\bar{\sigma}_{xx})_o$ is the amplitude of σ_{xx} at the surface. These ratios are plotted against Z/Λ, where Λ, as stated earlier, is the wavelentth of the vibrations. The curves illustrate clearly how the amplitude of the vibration in the x-direction passes through zero whereas the amplitude in the z-direction first increases slightly and then decays monotonically. They also show that σ_{xx} component changes sign, while the σ_{zz} component reaches a maximum at about $0.33/\Lambda$ and then decays asymptotically with depth.

CHAPTER IV

CONSIDERATIONS ON THE PROPAGATION OF SHOCKS THROUGH A PLASTIC MEDIUM

The preceding discussion in this report started with a consideration of the propagation of a shock and of the fluid flow in the shock-produced fluid. The compression by the shock is so great that the medium that was traversed by the shock front may be considered as an inviscid fluid, while the shock front propagates into the undisturbed solid. This report has continued with a discussion of the propagation of a shock front through a solid, elastic medium where there is no flow behind the shock front. There is an undetermined pressure range which exists between the elastic solid and the inviscid fluid region. This region is called a plastic medium and permanent distortion results from the passage of the shock. There is some flow, but the flow is against strong restraining forces.

This intermediate, plastic region is bounded on the low pressure side by the pressure at which permanent distortion of the medium starts to appear after the passage of the shock front. This subject is discussed at length in two sections that immediately follow this introduction. They are designated: (1) the Elastic and Dynamic Yield Strength and (2) the Bauschinger Effect under Shock Conditions. In the plastic range, there are believed to be two shocks that propagate at slightly different velocities. The upper limit of the plastic range may be

considered as the pressure at which the two shock fronts disappear. This is not a good criteria for two reasons. The so-called precursor shock becomes very small in the pressure range for which the plastic region merges into the fluid region. With the precursor amplitude very small, the small amplitude may not be sufficiently observable to determine the upper limit of the plastic region. There is another reason for confusion. The "fluid" shock, as contrasted to the precursor shock, propagates at a velocity that increases with pressure. As the pressure increases, the "fluid" shock may propagate at a velocity equal to, or faster than the precursor. In this case, the precursor shock would appear as a ripple on the oscillating shock front and would probably be overlooked.

Static and Dynamic Yield Strength of Metals

For sufficiently small strains the linear stress-strain relation (22),

$$\sigma_{ij} = 2\mu\epsilon_{ij} + \lambda(\epsilon_{11} + \epsilon_{22} + \epsilon_{33}) \qquad (1)$$

is applicable within an isotropic solid which is characterized by the density and by two elastic constants, μ, and λ. In Equation 1, σ_{ij} and ϵ_{ij} denote components of the Cartesian tensors for stress and strain, respectively.

For the case of one-dimensional compression in the x-direction, $\epsilon_{11} = \Delta V/V$ and all other $\epsilon_{ij} = 0$. By using Equation 1, the pressure along the x-direction, σ_{11}, is given by

$$\sigma_{11} = (2\mu + \lambda)\frac{\Delta V}{V}, \qquad (2)$$

whereas

$$\sigma_{22} = \sigma_{33} = \lambda \frac{\Delta V}{V} \tag{3}$$

Thus, the anisotropic part of the stress for the case of one-dimensional strain is

$$\sigma_{11} - \sigma_{22} = \sigma_{11} - \sigma_{33} = 2\mu \frac{\Delta V}{V} \quad \text{for } \sigma_{11} - \sigma_{22} < Y \tag{4}$$

where Y is the static yield strength in simple tension. The condition merely states that Equation 4 holds for stresses below the static yield strength.

For the case of a hydrostatic compression $\epsilon_{11} = \epsilon_{22} = \epsilon_{33} = \frac{1}{3} \frac{\Delta V}{V}$ and $\epsilon_{ij} = 0$ for $i \neq j$. By the use of Equation 1, it is seen that the associated stress tensor is

$$p = \sigma_{11}' = \sigma_{22}' = \sigma_{33}' = (\frac{2}{3} \mu + \lambda) \frac{\Delta V}{V} \tag{5}$$

$\sigma_{ij}' = 0$ for $i \neq j$.

An idealized stress-strain curve is shown in Figure 7. The presence of a cusp in the σ_{11} curve implies the position of the yield point, for the derivative of the offset, $\sigma_{11}' - \sigma_{11} = -\frac{4}{3} \mu \frac{\Delta V}{V}$ between this curve and the hydrostatic curve, suffers a discontinuity at Y. The hydrostatic curve is known to be smooth and to have no cusps. The pressure associated with the cusp is called the "Hugoniot elastic limit" or "dynamic elastic limit" (23).

Bauschinger Effect Under Shock Conditions

The Bauschinger effect is well known for heavily cold-worked metals. It is of interest to this discussion for it may increase the dynamic yield strength. The Bauschinger effect predicts that compressive loading of the metal to beyond the yield strength, by any means, will increase the original compressive yield strength, while it slightly

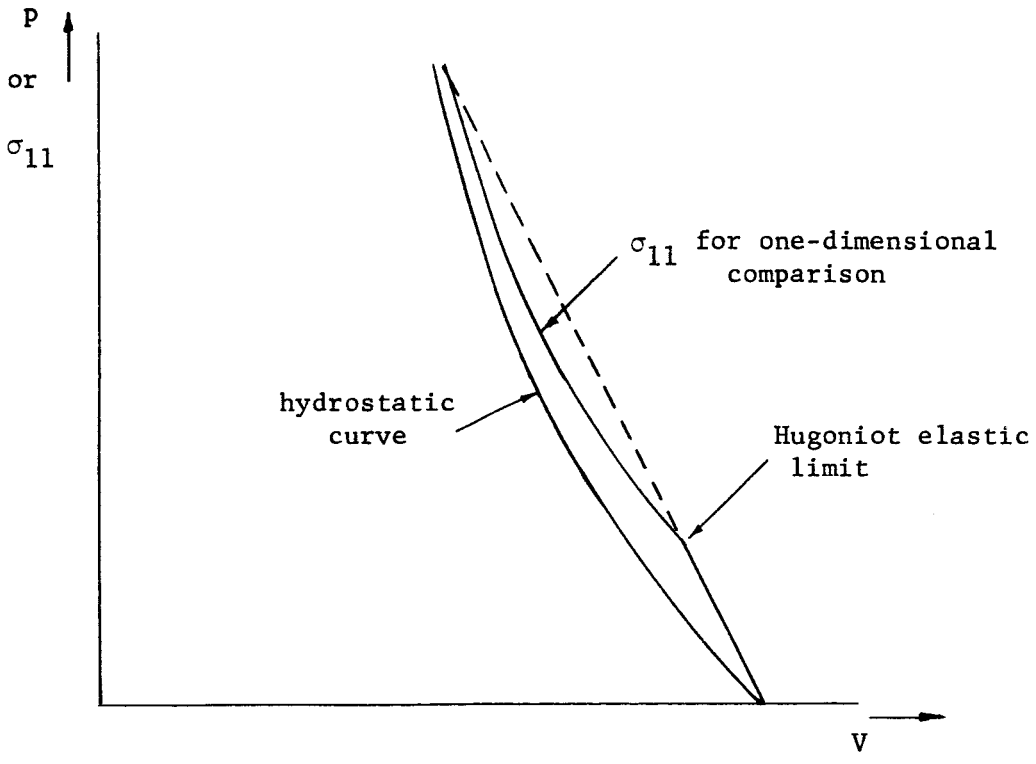

Fig. 7. Stress-Strain Curves for the Hydrostatic and One-Dimensional Compressions of an Isotropic Solid.

decreases the tensile yield strength. The early literature on shock loading has not reported a Bauschinger effect from shock loading at strain rates up to 10^6 sec^{-1}. It is to be recalled that the strain is expressed in cm/cm, so the only unit for the strain rate is reciprocal seconds. Jones and Holland (24) reported in 1964 that the Bauschinger effect is observed for mild steel under the extremely high strain rate that occurs in the explosive loading process. The following information is collected from their article.

The article by Jones and Holland clearly demonstrates that steel with 20 per cent of prior tensile cold work exhibits the Bauschinger effect. The results that demonstrate this result are reproduced in Figure 8. The experimental stress-time profile from the article are shown in Figure 9. The latter figure indicates the existence of a Bauschinger effect under explosive loading which results in very high strain rates. The modification from the Bauschinger effect on a one-dimensional elastic-plastic stress-strain path during a loading and unloading cycle was proposed. Their proposed cycle is reproduced in Figure 10, but they do not give a detailed, quantitative analysis. Under the conditions of the shock loading of mild steel, the experimental results are sufficient to show the Bauschinger effect for cold-worked mild steel under shock loading. From the preceding evidence, the Bauschinger effect may lead to serious errors. The conclusions from the cited article have several practical implications of a general nature. They are quoted:

> 1. If the dynamic yield strength of a meterial is to be accurately inferred from shock loading data given in the literature, care must be taken to duplicate the metallurgical history and the direction of loading. Unfortunately, this has not been given for more of the work reported in literature.

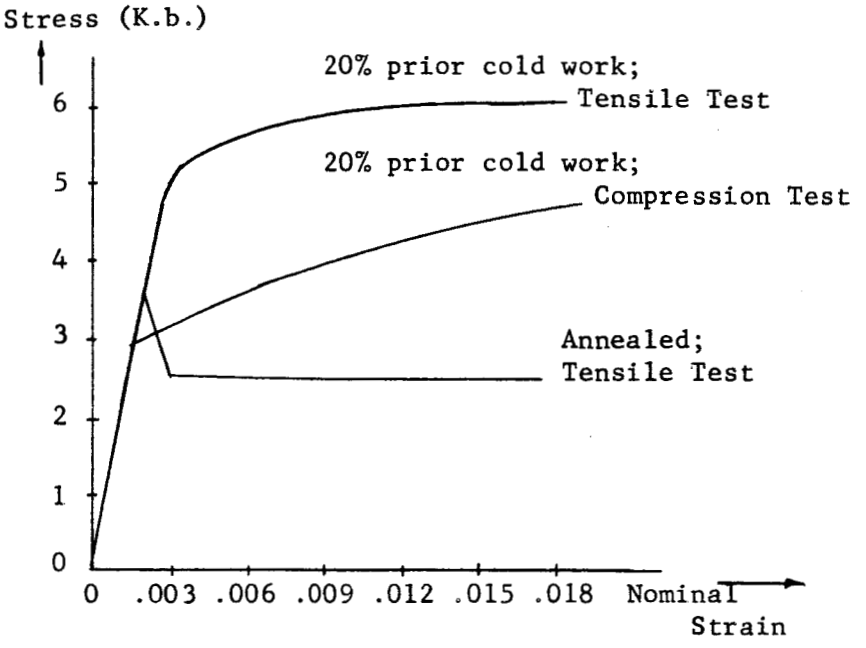

Fig. 8. Quasistatic Stress-Strain Curves for Annealed and Cold-Worked SAE 1018 Steel.

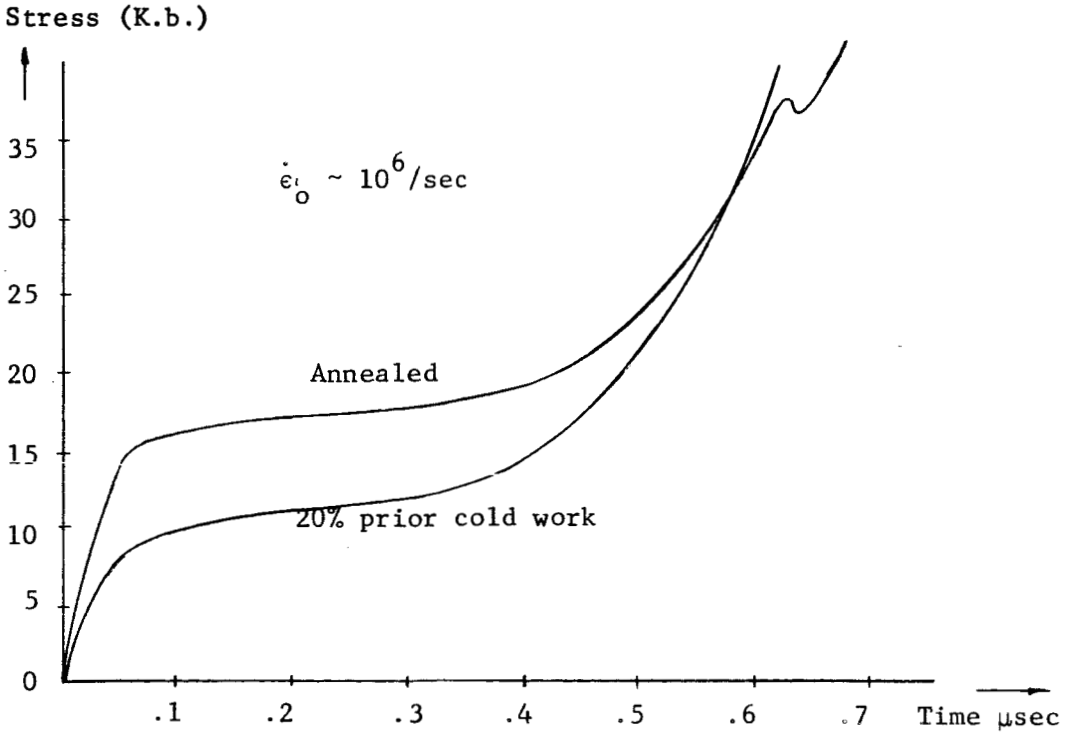

Fig. 9. Stress-Time Wave Profiles for Annealed and Cold-Worked SAE 1018 Steel Loaded Explosively in a State of One-Dimensional Strain. Specimens Nominally 1.905 cm Thick.

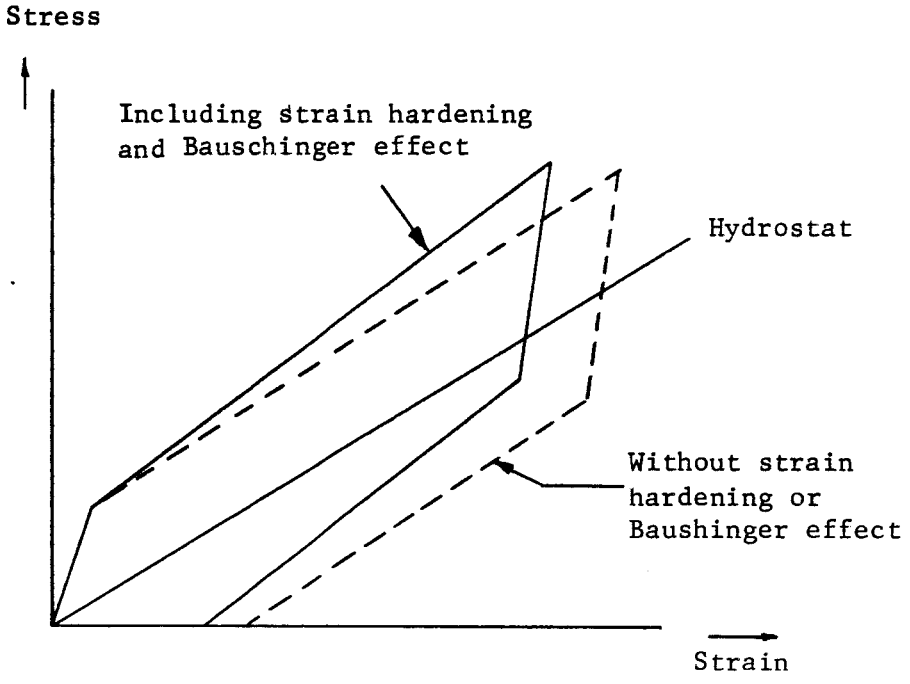

Fig. 10. Schematic Elastic-Plastic Stress-Strain Paths for Loading and Unloading in One-Dimensional Strain which Illustrates Modifications Resulting from Strain Hardening and the Baushinger Effect.

Alternatively, the Bauschinger effect may provide another experimental parameter which may be used to control the amplitude of the elastic wave profiles for a given metal.

2. In studying the stress-strain behavior of a metal under shock loading on the basis of free-surface measurements, it may be necessary to include the Bauschinger effect as shown in Figure 10, in the usual elastic-plastic theory of loading and unloading in one-dimensional strain. Such an effect has always been neglected in the past and would result not from prior deformation, but from work hardening during passage of the loading wave followed by reverse loading around the hydrostat.

Evidence for Existence of Two Successive Shocks

In the low pressure region, the behavior of the shock wave in a metal is determined by the yield strength of the metal. The shock structure depends on the final peak pressure reached in the compression. Because of the connection between the properties of the material and the structure of the shock front, the investigation of this structure increases the amount of information that can be obtained from shock experiments. The connection between the shock structure and material properties is not always unique, and possible alternative interpretations must be carefully weighed (25). The first concept to be abandoned is that the shock pressure is a simple hydrostatic pressure, as would occur in an ideal fluid. The compression by a relatively small shock of any material with a definite yield strength must be calculated by the use of stress tensors. If the smallest element for consideration with a practical structural metal consists of several crystals, the stress tensor must be isotropic. The shock compression allows no net macroscopic strain to occur immediately behind and parallel to the shock front. The Rankine-Hugoniot jump conditions show that measurements of the propagation velocity and of the normal component of particle

velocity give information only about the component of compressive stress normal to shock front. These considerations lead to the conclusion that the stress parallel to the wave front is essentially unknown, except by inference from other information that may be combined with the velocity measurements (26).

For consideration of shock stability, the yield point has the same effect as a phase transition (27). The stability of a shock transition may be tested, in general, by connecting the initial and the final state of the material on its Hugoniot curve by a straight line. If the line does not intersect the Hugoniot at intermediate points, the shock transition is stable, otherwise it is not. The most direct evidence of the existence of two successive shock waves is the motion of the free surface that results from the incidence of the shock wave (28). The velocity from a single shock is essentially constant, as is shown in Figure 11 (29). The deceleration results from the finite tensile strength of the material and the decay behind the incident shock. If, in Figure 12, P_1 lies above point B_1 only a single shock is formed. The shock velocity, in this case, can be found by eliminating the particle velocity from Equations 1 and 2 in Chapter I. If, again in Figure 12, P_1 lies below point A, which is the dynamic elastic limit of the material, a single elastic compression occurs. If P_1 is between points A and B, the shock consists of an elastic precursor of amplitude P_A followed by a slower moving shock with peak pressure, P_1. The case is shown in Figure 13. For this case, the pressure between the elastic precursor and the shock is shown as constant. This holds for a sharp yield point and for a constant yield stress in simple tension. The velocity of a single shock with a peak pressure, P_1, above point B in

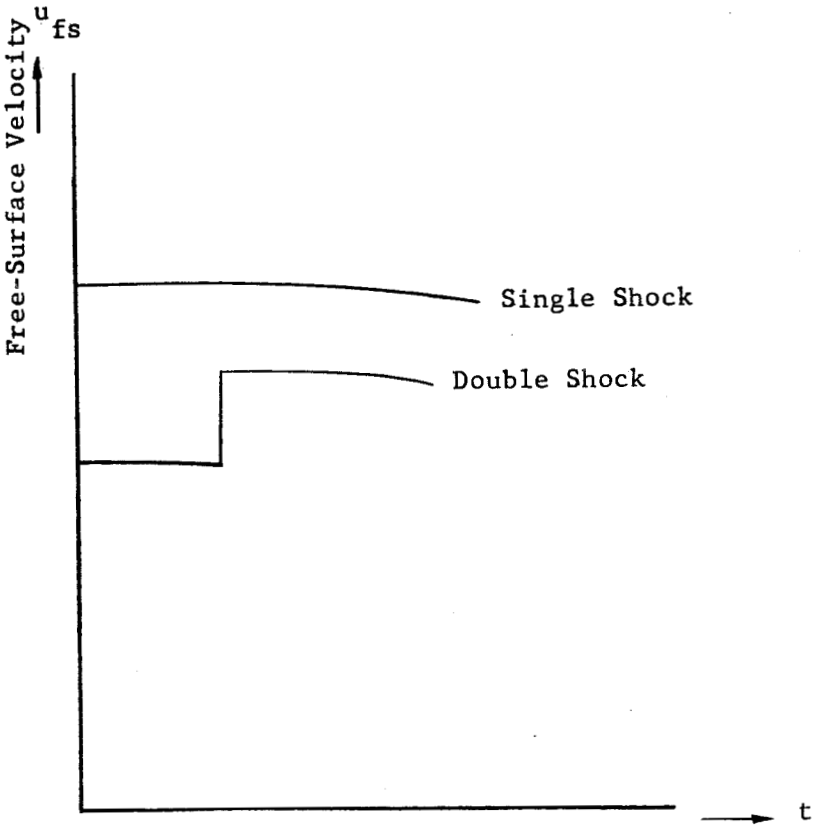

Fig. 11. Free-Surface Velocities Produced by Single and Double Shock.

Figure 12, is given by

$$U = V_o \left[\frac{P_1 - P_o}{V_o - V_1}\right]^{\frac{1}{2}} \tag{5}$$

which is proportional to the square root of the negative slope of the chord drawn between the points representing the initial, and the final state on the Hugoniot curve (30). The velocity of the elastic precursor, U_e, can be shown to be equal to

$$U_e = \left[\frac{3K}{\rho}\frac{(1 - \upsilon)}{(1 + \upsilon)}\right]^{\frac{1}{2}}, \tag{6}$$

where K is the bulk modulus of compression, ρ the density of the material and υ is Poison's ratio (31).

For the case of double wave structure that was mentioned earlier, the velocity of the elastic precursor, P_A, is again given by Equation 6. Since P_1 is above the dynamic elastic limit, plastic flow occurs and is propagated with the plastic wave velocity

$$U_p = (K/\rho)^{\frac{1}{2}}, \tag{7}$$

where K is again the bulk modulus of the material. As mentioned earlier, Bridgman showed that for most solids, the bulk modulus K increases with increasing pressure. At stresses only slightly greater than the dynamic elastic limit, the plastic wave velocity from Equation 7 is smaller than that of the elastic wave given by Equation 6. However, as the applied stress increases, the plastic wave velocity also increases because of the decreasing of compressibility of the material. As a result of this, further increase of pressure causes the plastic wave velocity to exceed that of the elastic wave. A pressure exists at which the plastic wave velocity becomes equal to that of the elastic wave. For aluminum this

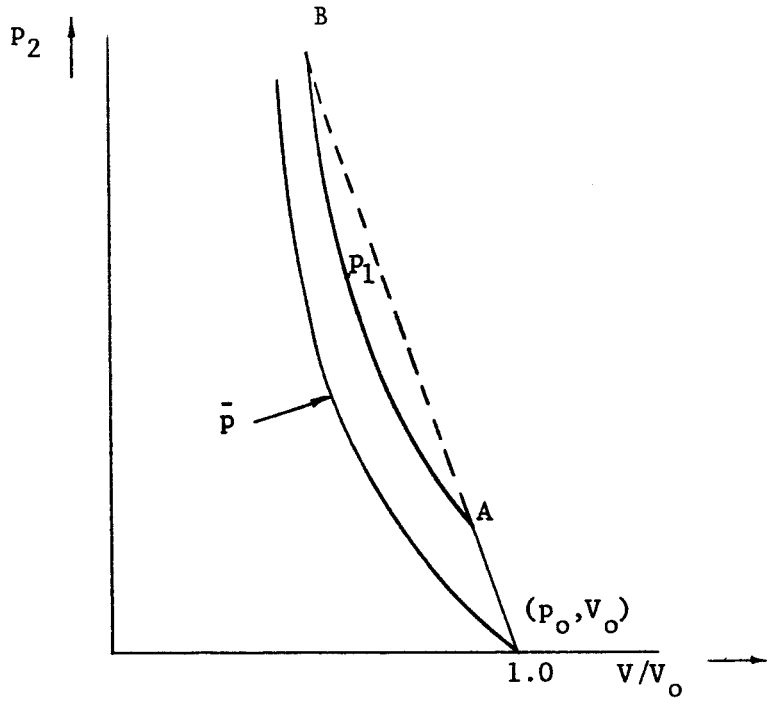

Fig. 12. Equation of State in Elastic-Plastic Solid.

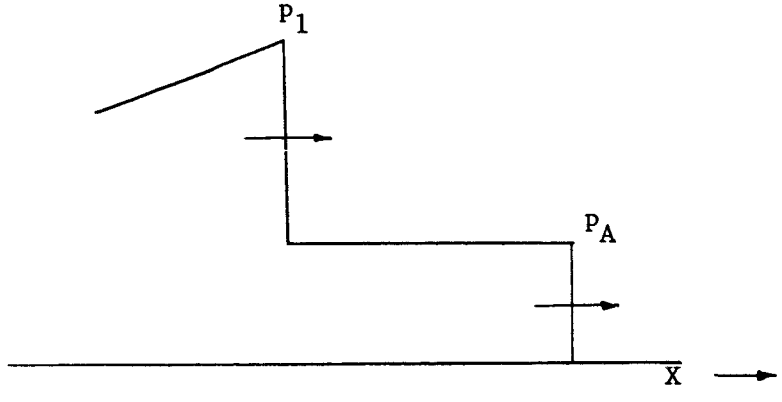

Fig. 13. Shock Structure in Elastic-Plastic Solid.

pressure is about 105 Kilobars (32). The material is in the elastic region for pressures under the dynamic elastic limit.

An elastic precursor shock was reported to precede an explosively generated shock wave in steel by Pack, Evans and James (31) in 1948. Later studies by other investigators have measured the amplitude of this wave for various materials (33,34) and several theories have been formulated for shock waves in materials which may be deformed plastically (35,36,37). Dynamic yield strength for compressive elastic waves have been derived from the shock wave experiments and compared with tensile experiments. Generally, the results support the hypothesis that dynamic, compressive yield occurs by the same mechanisms as yield in tension. Calculation of the dynamic elastic limit for a plastic material with fixed yield stress indicate that it exceeds the hydrostatic value at a given strength by two-thirds of the yield stress (38).

Equation of State for Aluminum in Low Pressure Region

As an example of shock loading, consider a plane, uniform, compressional shock wave which propagates in a uniform material as shown in Figure 14. A small element of volume in the medium with cross-section ABCD is compressed into A'B'C'D', as a result of application of the pressure, P_x, in x-direction. The application of a one-dimensional compression P_y requires a pressure $P_z=P_y$ to prevent an expansion or a contraction on the sides of the volume element. A material is called "elastic-plastic" provided (1) it yields according to the von Mises-Hencky criterior and (2) it is elastic at lower stresses. The von Mises-Hencky criterior is $P_x-P_y = \sigma_y$ where σ_y is

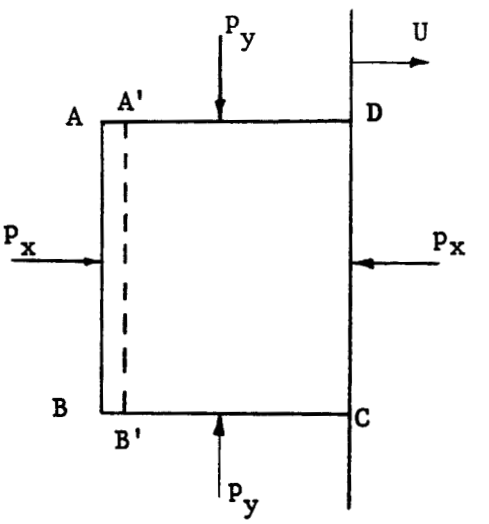

Fig. 14. Compression of a Volume Element by a Plane Shock Front.

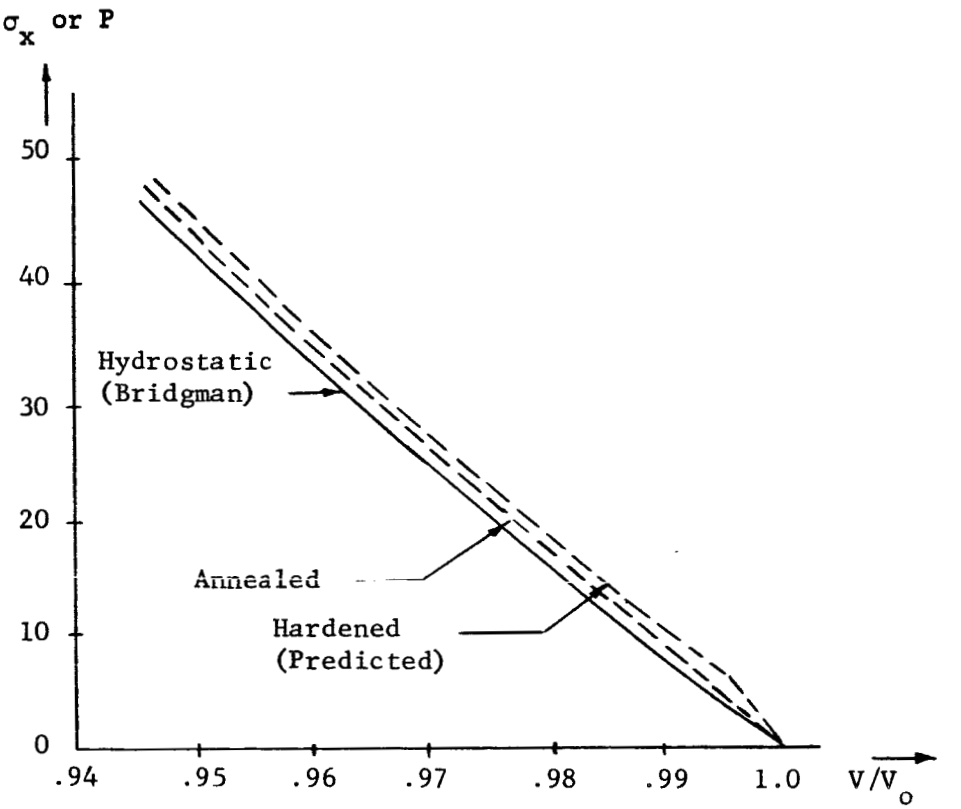

Fig. 15. Hugoniots for Hydrostatic and Elastic-Plastic Compression of Aluminum.

the yield strength in simple tension.

A Hugoniot relation for such a material can be readily constructed, if strain rate effects are neglected. While the compressed material behaves elastically, compressive stresses and strains are related by Hooke's law:

$$P_x = (\lambda + 2\mu)\epsilon_x \tag{8}$$

$$P_y = \lambda\epsilon_x \tag{9}$$

$$P_z = \lambda\epsilon_x \tag{10}$$

where $\epsilon_1 = 1 - \rho_o/\rho$, and λ, μ are the Lame's elastic constants. By definition,

$$\bar{P} \equiv \frac{1}{3}(P_x + P_y + P_z) = (\lambda + \frac{2}{3}\mu)\ \epsilon_x \equiv K\epsilon_x \tag{11}$$

where K is the bulk modulus of the material.

By combining the relations in Equation 8 and 11, the following equation is obtained.

$$P_x = (K + \frac{4}{3}\mu)\epsilon_x = (K + \frac{4}{3})(1 - \rho_o/\rho) \tag{12}$$

where μ is the modulus of rigidity. While the compressed material is in the plastic state, the plastic stress function in simple tension is $P_x - P_y = \sigma_y(\epsilon^P)$. Insert this relation in Equation 11 and obtain the relation,

$$\bar{P} = P_x = \frac{2}{3}\sigma_y(\epsilon^P) \tag{13}$$

In terms of $\bar{P}$ and σ_y, P_x may be expressed by

$$P_x = \bar{P}\ (\rho_o/\rho) + \frac{2}{3}\sigma_y\ (\epsilon^P) \tag{14}$$

where $\bar{P}(\rho_o/\rho)$ is the hydrostatic pressure corresponding to density ρ and ϵ^P is the equivalent plastic strain in simple tension. The normal

stress, P_x, in the plane wave exceeds the hydrostatic pressure corresponding to the same density by an amount depending on the yield stress. The plastic strain corresponding to the stress, P_x, is the difference between the elastic strain that is required to resist the stress, P_x, and the total strain produced by P_x. The resulting equation may be readily solved, graphically. If $\sigma_y(\epsilon^P)$ is a constant, the locus of elastic-plastic states lies above the hydrostatic pressure by $\frac{2}{3}\sigma_y$. The P-V diagram for hydrostatic and elastic-plastic compression of aluminum (38) is shown in Figure 15.

By different experimental techniques from those of G. R. Fowles (38), Lundergan and Hermann (32) were able to formulate an impirical equation of state for aluminum in the low pressure region. Their equation has the following form for stress below the dynamic elastic limit:

$$P = 1044 \left(\frac{\Delta V}{V_o}\right)$$

where P is in Kilobar.

Beyond the dynamic elastic limit the equation has the following form:

$$P = 744 \left(\frac{\Delta V}{V_o}\right) + 1.6,$$

where P is again in Kilobar.

CHAPTER V

HUGONIOT CURVE FOR SPECIAL MATERIALS

The Hugoniot curve has been defined for metals as the locus of points on the P-V plot to which a material is compressed by shock waves. Compression by a shock is the principal experimental technique that is employed to obtain information on the equation of state of metals at high pressures, densities and temperatures. A shock compression from a single, initial value of the density gives a single point on the P-V diagram and the entropy increases with amplitude of the shock. Shock compressions, for a series of samples with different initial densities, yield more data and a complete region of the P-V diagram may be constructed (41). Compression to a selected point on the P-V diagram gives a compressed state at high temperatures as the initial porosity is increased. The simplest method to obtain various initial densities is to prepare sample with different porosities from fine powder. The fractional porosity, m, of a metal is defined as $m = \rho_o/\bar{\rho}$, where ρ_o is the density of solid-metal particles of the sample and $\bar{\rho}$ is the mean density of the whole porous sample.

Heating Effect with Porous Metals

In a typical porous material, individual particles of solid matter of normal density, ρ_o, are separated by empty spaces. In shock compression, the work done by the external pressure is first used to

compress the porous metal to a solid. A shock wave of low intensity can compress porous matter to a solid matter of normal density. For the final pressures equal the density after shock compression is smaller for a porous material than for a nonporous one. The final density decreases as the initial porosity increases. This is a consequence of the greater heat content of the compressed porous material. The physical explanation is shown in Figure 16. The path along which work is done by the shock-compression forces on the proous material is longer than the corresponding path for the nonporous material. Since half of the work is needed to increase internal energy, the increase in the thermal component, E_T^p, of the internal energy of a porous material is considerably larger than the corresponding quantity, E_T^n, for the nonporous material. The additional temperature rise from the porosity of the material increases the thermal component of the pressure, $P_t = P - P_c$, which opposes the compression. As a consequence of greater heat input, the density of a shock-compressed, porous sample is lower than that of a nonporous sample under the same shock amplitude.

The shock compression of samples of the same material with different initial porosities was first considered theoretically by Ya. B. Zel'dovich and A. S. Kompaneets. They used an equation of state with a constant coefficient, $\gamma = V(\frac{\partial P}{\partial E})_V$. Their results are shown in Figure 17 by pressure-relative density ($\eta = \rho/\rho_o$) diagram. Shock compression curve of the nonporous material, with m = 1, and of samples with various initial proosities, m > 1, all start from the point P = 0, η = 1, which is the initial state of the nonporous material. This results from the assumption that a very weak shock is capable of compressing a porous material so that its density becomes ρ_o.

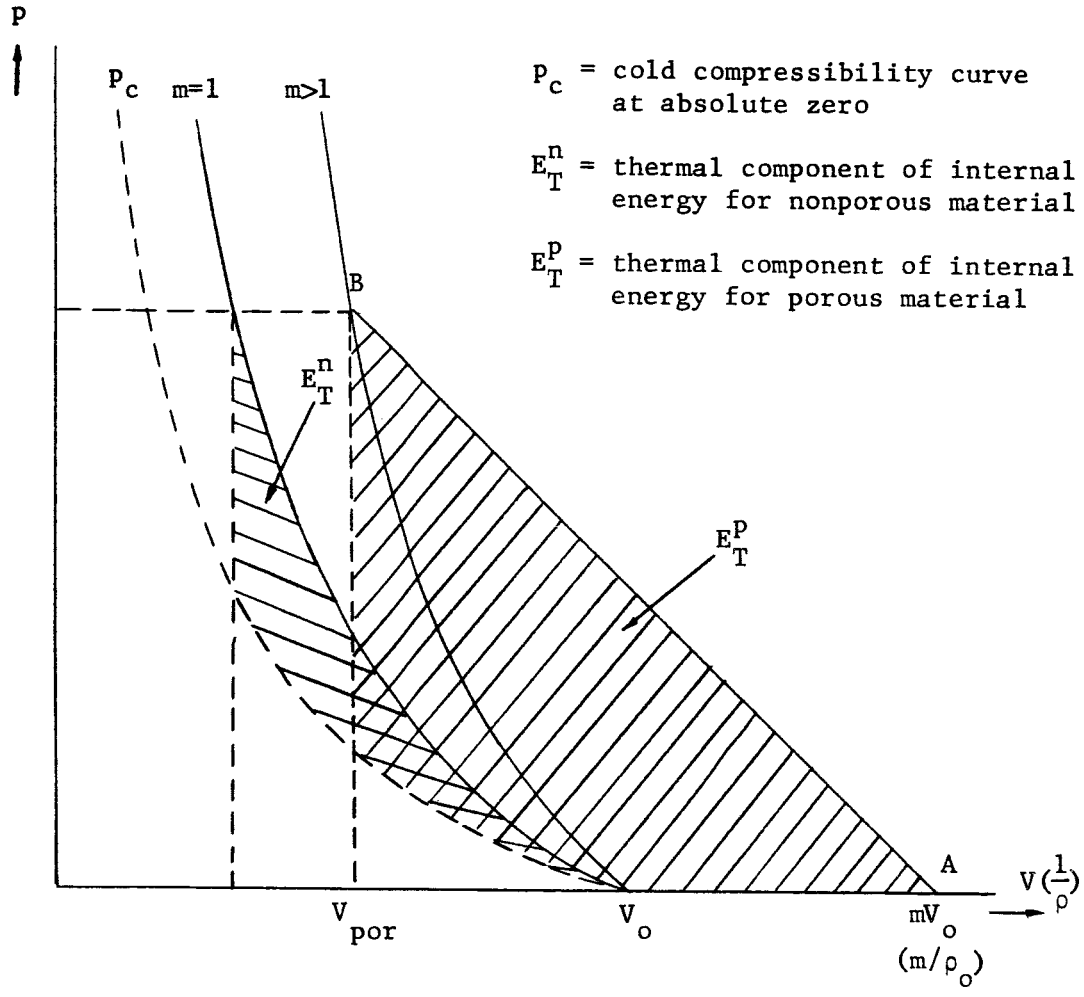

Fig. 16. The P-V Diagram for Shock Compression of Porous Material.

For higher values of m, the compressive shock shifts the curves in the P-η diagram in Figure 17 toward lower value of η. Let $h = 1 + 2/\gamma$ denote the limiting compression of a nonporous body as P increases indefinitely. For the shock compression curves corresponding to a porosity, m, in the interval $h > m_1 > 1$, the density after shock compression increases with an increase of the pressure, approaching asymptotically to a limiting value, $\eta_{1im} = \frac{h}{m} > 1$. These curves lie in the region, $\eta > 1$, where their slopes, $(\frac{dp}{d\eta})_H$, are positive. The effect of shock heating is particularly remarkable at the porosities, $m_3 > h$. In this case, the shock compression curves have an unusual, inverted form. They lie in the region and may have derivatives, $(\frac{dp}{d\eta})_H < 0$. A shock wave of vanishingly small amplitude is capable of compressing a porous sample to the normal density of the nonporous material. When $m > h$, a wave of finite amplitude cannot produce this much compression. An increase in pressure produces a decrease in the density instead of the increase in density that might be expected. The density after shock compression approaches asymptotically to a limiting value of $\eta_{1im} = \frac{h}{m_3} < 1$. When the porosity $m = m_2 = h$, the shock compression curve coincides with the ordinates $\eta = 1$ along which $(\frac{dp}{d\eta})_H = \infty$. The shock compression curves for porous tungsten with various porosities and those for iron with m = 1.4 are shown in Figure 18 and Figure 19, respectively.

Hugoniot for Marble

A shock adiabat for marble was reported by Dremin and Adadurov (42) in 1959. A light-gray marble was used which had an initial density of 2.70 gm/cm^3. The following results were obtained. The shock

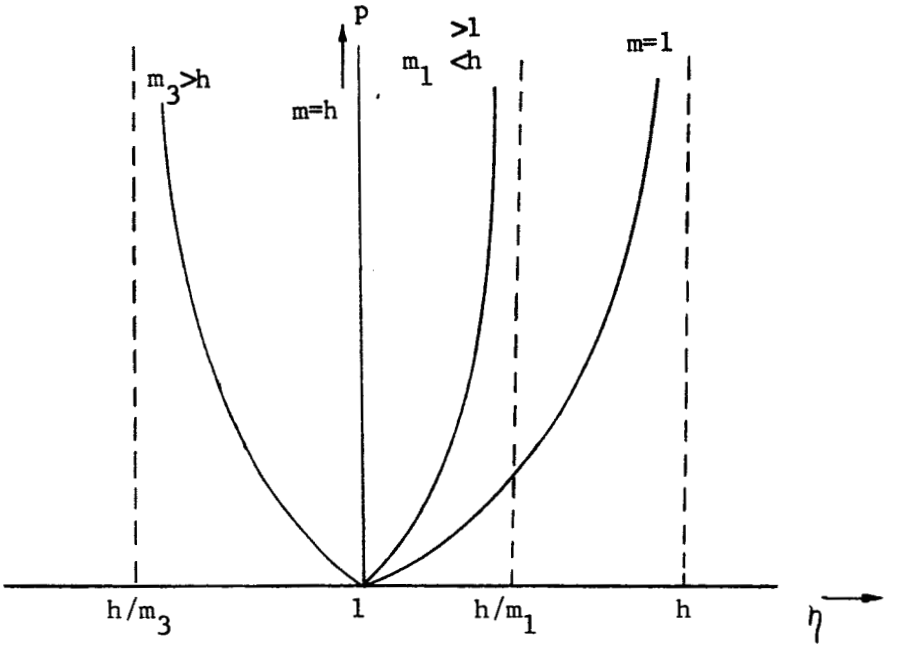

Fig. 17. Compression of Porous Samples for Various Values of h/m with $h = 1 + 2/\gamma$.

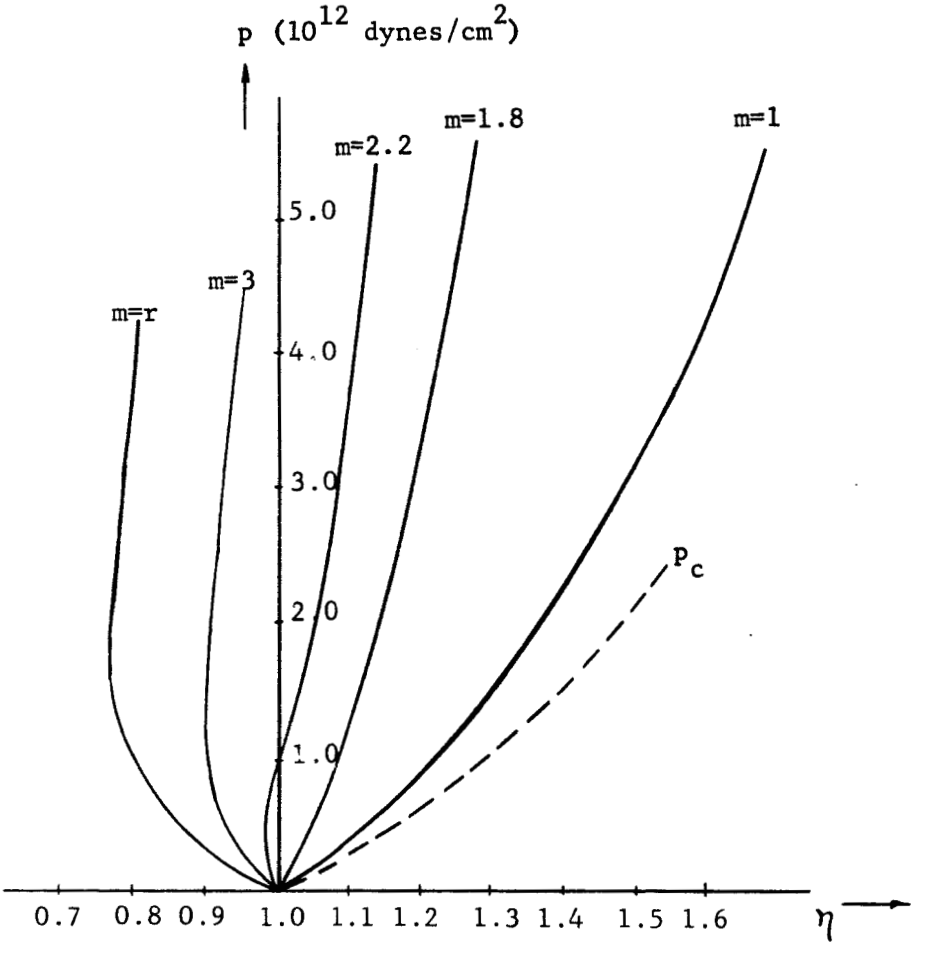

Fig. 18. Shock Compression Curves for Porous Tungsten.

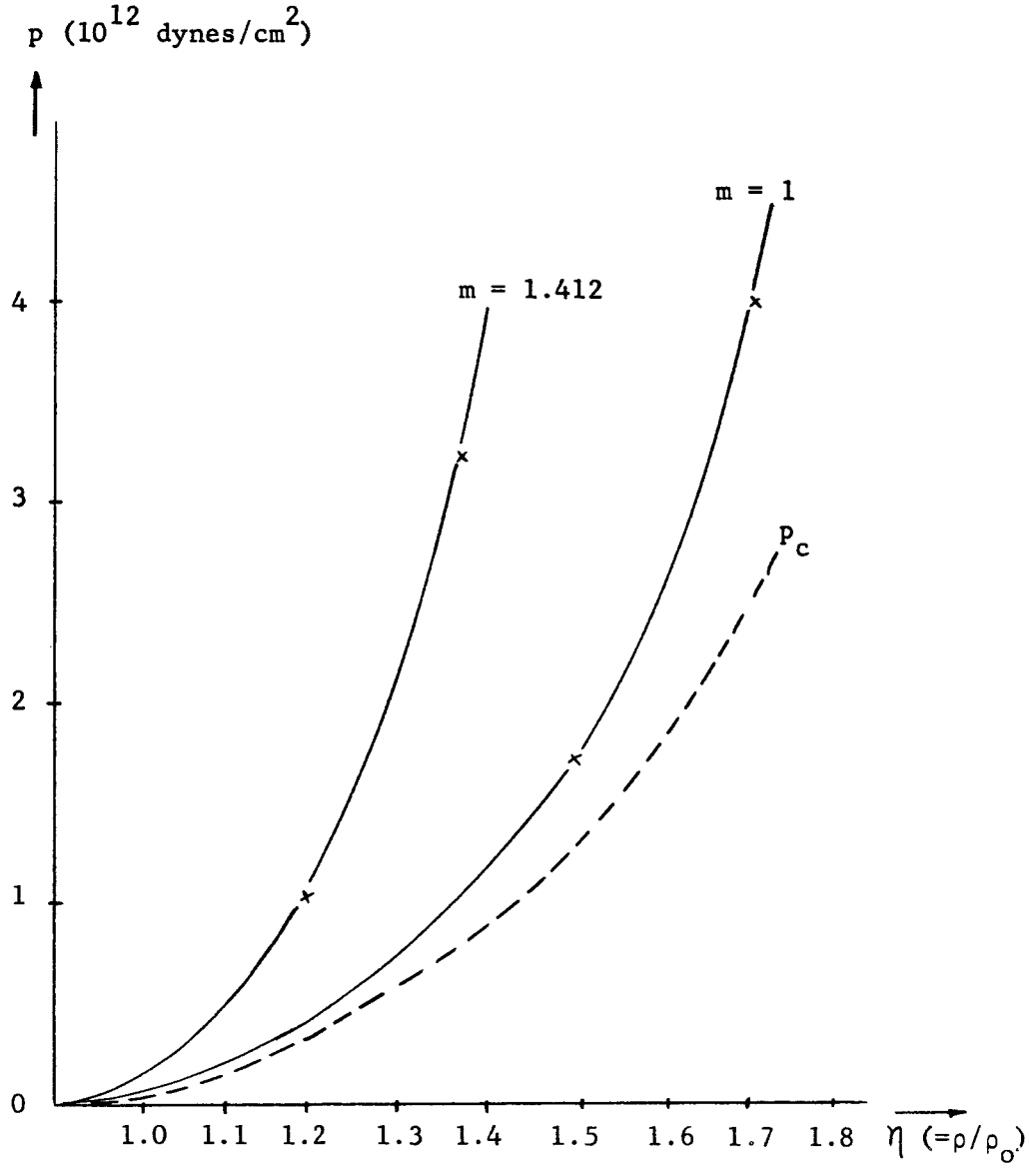

Fig. 19. Shock Compression Curves of Iron with Normal Density m=1, and Porosity m = 1.412.

pressure extends up to 500 Kilobars.

The dependence of the shock wave velocity, U, on the particle velocity, u, is shown in Figure 20. The Hugoniot with pressure vs. the ratio of the density under compression to normal density is given in Figure 21. There is a remarkable discontinuity in the U vs. u curve at about u = 1,000 m/sec, as shown in Figure 20. This is attributed to a phase transition. The segment AB on Figures 20 and 21 corresponds to a region of mixed phase. The boundaries of this region were established. As was shown by Drummone (43), Bancroft, Peterson, and Minshall (34), a configuration of two shock waves exists in the phase-transition region. The disturbance of the first shock wave was measured experimentally. It was found to propagate in the entire phase-transition region at a constant velocity which is greater than the velocity of the second shock wave. With increasing pressure amplitude, the velocity of the second shock wave becomes larger and larger; and, eventually, at pressures corresponding to point B in Figure 21, the velocity of both shock waves becomes equal. With a further increase of the pressure, only one shock wave propagates in the material.

Two empirical equations are found. One gives the relation of the pressure, P, to the density ratio, ρ/ρ_o and this is the Hugoniot equation of state for marble. The other equation relates the shock wave velocity, U, and the particle velocity, u. The match of experiment to empirical data is shown in Figures 21 and 20. Up to the phase-transition region, these relations have the form

$$P = 42.6 \times 10^9 \left[(\rho/\rho_o)^{7.23} - 1\right]$$

where P is in bars:

$$U = (3.39 + 2.0u)$$

where both U and u are in km/sec. After phase-transition the relations have the form

$$P = 106 \times 10^9 \left[(\rho/\rho_o)^{4.1} - 1\right] \text{ bars.}$$

$$U = (4.01 + 1.30u) \quad \text{km/sec.}$$

In order to determine the boundary of the phase-transition region without considerably increasing the amplitude of the shock wave, the point at which a further increase in pressure brought no change in the shock wave velocity in the marble was found. This velocity is equal to 5.40 km/sec. The intersection of the straight line U = 5.4 km/sec with the U-u curve in Figure 20 gives the boundary points, A and B. The corresponding pressure at the point A is equal to 146.5 Kilobars, while $\rho/\rho_o = 1.230$. At point B, the corresponding pressure is equal to 155.8 Kilobars with $\rho/\rho_o = 1.247$.

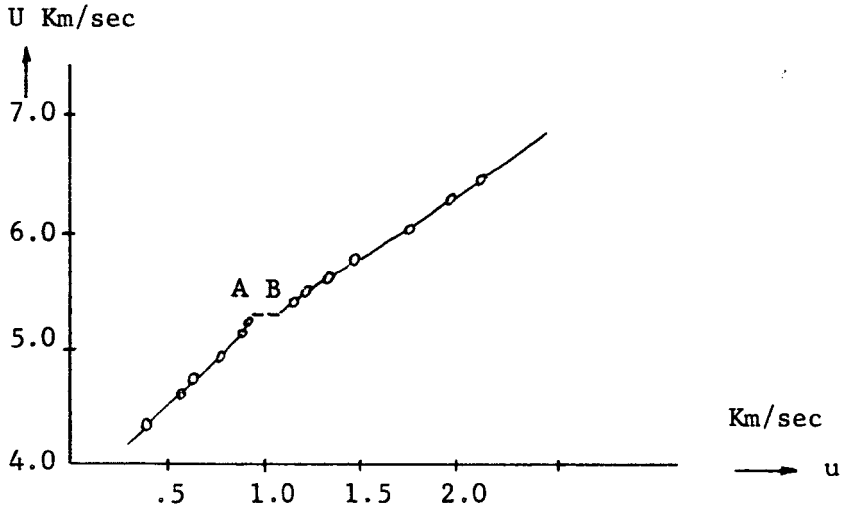

Fig. 20. Dependence of the Shock Wave Velocity U on the Particle Velocity u. A-Segment up to the Phase Change; B-Segment After Phase Change; Mixed Phase Region Between A and B.

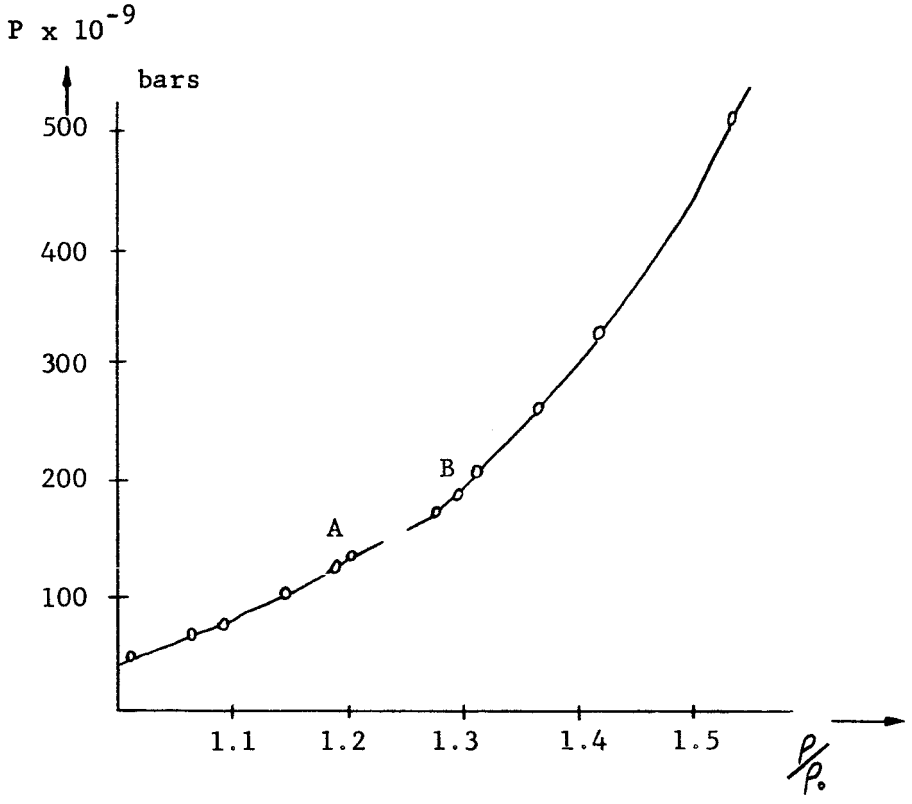

Fig. 21. Shock Compression Curve of Marble. A-Segment up to the Phase Change; B-Segment After the Phase Change; Mixed Phase Region Between A and B.

SELECTED BIBLIOGRAPHY

1. Bethe, H. A. OSRD No. 545, Division B of National Defense Research Committed "The Theory of Shock Waves for an Arbitrary Equation of State."

2. Bjork, R. L. J. Geophys. Res. 66 (1961) 3379.

3. von Neumann, J. and R. D. Richtmyer. J. Appl. Phys. 21 (1950) 232.

4. Courant, R. and K. O. Friedrichs. Supersonic Flow and Shock Waves. New York: Interscience Publishers (1948).

5. Bleakney, W., and A. H. Tauk. Rev. Mod. Phys. 21 (1949) 584.

6. l. c. 4, p. 121, p. 134.

7. Band, Wm., and G. E. Duvall. Amer. J. Phys. 29 (1961) 780.

8. Rice, N. H., R. G. McQueen and J. M. Walsh. Solid State Physics, Advances in Research and Applications. New York: Academic Press (1958) 1.

9. l. c. 4, p. 141.

10. Duvall, G. E., and B. J. Zwolinski. J. Accoust. Soc. Amer. 27 (1955) 1054.

11. Walsh, J. M., N. H. Rice, R. G. McQueen and F. L. Yarger. Phys. Rev. 108 (1957) 196.

12. l. c. 8, p. 1.

13. Bjork, R. L. J. Geophys. Res. 66 (1961) 3379.

14. l. c. 4, p. 12.

15. Richtmyer, R. D. Difference Methods of Initial-Value Problems. New York: Interscience Publishers (1957) 207.

16. l. c. 15, p. 208.

17. l. c. 15, p. 210.

18. Bridgman, P. W. The Physics of High Pressure (1931).

19. Love, A. E. H. A Treatise on the Mathematical Theory of Elasticity. University Press, Cambridge (1927).

20. Broberg, K. B. Shock Waves in Elastic and Elastic-Plastic Media. Stockholm: (1956) 93.

21. Kolsky, H. Stress Waves in Solids. New York: Dover Publications, Inc., (1963) 16.

22. Sokolnikoff, I. S. Mathematical Theory of Elasticity. New York: McGraw-Hill Co. (1946).

23. 1. c. 8, p. 1.

24. Jones, O. E. and J. R. Holland. J. Appl. Phys. 35 (1964) 1771.

25. Bradley, R. S. High Pressure Physics and Chemistry. New York: Academic Press (1963) Vol. 2, p. 255.

26. 1. c. 25, p. 255.

27. 1. c. 25, p. 258.

28. Duvall, G. E. Response of Metals to High Velocity Deformation. New York: Interscience Publishers (1961) 165.

29. 1. c. 28, p. 188.

30. 1. c. 8, p. 1.

31. Pack, D. C., W. M. Evans, and H. J. James. Proc. Phys. Soc. 60 (1948) 1.

32. Lundergan, C. D., and W. Hermann. J. Appl. Phys. 34 (1963) 2046.

33. Goranson, R. W., D. Bancroft, B. L. Vurton, T. Blecher, E. E. Houston, E. F. Fittings, and S. A. Landeen. J. Appl. Phys. 26 (1955) 1472.

34. Bancroft, D., E. L. Peterson, and S. Minshall. J. Appl. Phys. 27 (1956) 291.

35. Wood, D. S. J. Appl. Mech. 19 (1952) 521.

36. Morland, L. W. Phil. Trans. Roy. Soc. London, A251 (1959) 341.

37. Broberg, K. B. Shock Waves in Elastic and Elastic-Plastic Media. Stockholm: (1956).

38. Fowles, G. R. J. Appl. Phys. 32 (1961) 1475.

39. Kmpnikov, K. K., M. I. Brazhnik and V. P. Krupnikova. Soviet Phys. JETP 15 (1962) 470.

40. Altshuler, L. V., K. K. Krupnikov, B. L. Ledenev, V. I. Zhuchikhin and M. I. Brazhnik. Soviet Phys. JETP 7 (1958) 606.

41. Zel'dovich, Ya. B. Soviet Phys. JETP 5 (1957) 1103.

42. Dremin, A. N. and G. A. Adadurov. Soviet Phys "Doklady" 4 (1959) 970.

43. Drummond, W. E. J. Appl. Phys. 28 (1957) 998.

VITA

Lin Wang

Candidate for the Degree of

Master of Science

Report: ANALYTICAL CONSIDERATION ON THE PROPAGATION OF A SHOCK THROUGH FLUID, PLASTIC AND ELASTIC MEDIA

Major Field: Physics

Biographical:

Personal Data: Born at An-Tung, Republic of China, June 11, 1929, the son of Lu-Ting and Shou-Jean Wang.

Education: Graduated from the Second High School of the City of An-Tung, China. Earned B.S. degree in physics in 1956 from National Taiwan University, Taipa, Taiwan, China.

Professional Experience and Organizations: Assistant Teacher in Physics Department, Provincial Chang-Kung University, Tainan, Taiwan, China. Research Assistant for the Oklahoma State University Research Foundation. Member of Sigma Pi Sigma.